

**T.C**  
**BOLU ABANT IZZET BAYSAL UNIVERSITY**  
**THE GRADUATE SCHOOL OF NATURAL AND APPLIED**  
**SCIENCES**



**PRODUCTION OF CARBON DOPED BORON TO**  
**SYNTHESIZE HIGH PERFORMANCE MgB<sub>2</sub>**  
**SUPERCONDUCTOR**

**MASTER OF SCIENCE**

**EMİR PİLTEN**

**BOLU, AUGUST 2019**

**T.C**  
**BOLU ABANT İZZET BAYSAL UNIVERSITY**  
**THE GRADUATE SCHOOL OF NATURAL AND APPLIED**  
**SCIENCES**  
**DEPARTMENT OF PHYSICS**



**PRODUCTION OF CARBON DOPED BORON TO**  
**SYNTHESIZE HIGH PERFORMANCE  $MgB_2$**   
**SUPERCONDUCTOR**

**MASTER OF SCIENCE**

**EMİR PİLTEN**

**BOLU, AUGUST 2019**

## APPROVAL OF THE THESIS

**PRODUCTION OF CARBON DOPED BORON TO SYNTHESIZE HIGH PERFORMANCE  $MgB_2$  SUPERCONDUCTOR** submitted by **EMİR PİLTEN** in partial fulfillment of the requirements for the degree of **Master of Science** in **Department of Physics, The Graduate School of Natural and Applied Sciences of BOLU ABANT İZZET BAYSAL UNIVERSITY** in **02/08/2019** by

### Examining Committee Members

### Signature

Supervisor  
Prof. Dr. İbrahim BELENLİ  
Bolu Abant İzzet Baysal University

*Belentli*

Member  
Prof. Dr. Mehmet SOMER  
Koç University

*Somer*

Member  
Prof. Dr. Hakan YETİŞ  
Bolu Abant İzzet Baysal University


*Yetiş*

Prof. Dr. Ömer ÖZYURT

*Özyurt*

Director of Graduate School of Natural and Applied Sciences

✓



To my family

## **DECLARATION**

I hereby declare that all information in this document has been obtained and presented in accordance with academic rules and ethical conduct. I also declare that, as required by these rules and conduct, I have fully cited and referenced all material and results that are not original to this work.

**Emir PİLTEN**



## ABSTRACT

### PRODUCTION OF CARBON DOPED BORON TO SYNTHESIZE HIGH PERFORMANCE $MgB_2$ SUPERCONDUCTOR

MSC THESIS

EMİR PİLTEN

BOLU ABANT İZZET BAYSAL UNIVERSITY GRADUATE SCHOOL OF  
NATURAL AND APPLIED SCIENCES

DEPARTMENT OF PHYSICS

(SUPERVISOR: PROF. DR. İBRAHİM BELENLİ )

BOLU, AUGUST 2019

$MgB_2$  has been known almost six decades although its superconductive property is discovered only in 2001. Since then the usage in superconductive wires, coils and magnets became quite common due to its convenience and cost-effective availability.  $MgB_2$  is a unique superconductor when it comes to critical temperature ( $T_c = 39$  K) occupying middle place between the so called low temperature (LT) superconductors (e.g. NbTi, 9K) and the high temperature BSCCO (Bismuth strontium calcium copper oxide) which is 108 K.

Superconductors need to reach these critical temperatures in order to work efficiently.  $MgB_2$  can be easily cooled by the usage of liquid hydrogen or solid state nitrogen/cryocooler that is readily available at a significant cost difference.

In this study we aimed to improve the superconductivity properties of  $MgB_2$  by doping with different carbon containing sources (sugar and malic acid) at mass percentages of 3, 6 and 9. In the preliminary experiments, malic acid and sugar were decomposed under thermogravimetric conditions (DTG, Ar) and the weight changes, the temperature of decomposition and formation of pure carbon (ca. 400 °C) were determined. The addition of Mg at this stage is not favorable due to presence of the water which forms during the decomposition of the precursor's malic acid and sugar. The phase purity of the samples was analyzed by X-Ray diffraction method. For the determination of the lattice constants in each sample Rietveld analysis performed. To obtain numerical precession from the XRD the measured reflections were calibrated with the well-known Si standard. The results show the expected shifts in the lattice parameters  $a$  and  $c$  axes with respect to the pure  $MgB_2$ . Very typical hereby is the increase of the  $c/a$  ratio in the doped specimen proportional to the amount of C insertion into the lattice of  $MgB_2$ . Starting from the same nominal carbon contents, the doping with sugar is more effective than when malic acid was employed as C-precursor. We believe that this is directly related to the homogeneity of the reactants - and particularly to that of carbon - in the overall process.

**KEYWORDS:**  $MgB_2$ , Malic Acid, Critical Temperature, Superconductor , Ball Milling , Reitveld Analysis, Lattice Parameter

## ÖZET

**YÜKSEK PERFORMANSLI  $MgB_2$  ÜRETİMİ İÇİN KARBON  
KATKILANMIŞ BOR SENTEZİ  
YÜKSEK LİSANS TEZİ  
EMİR PİLTEN  
BOLU ABANT İZZET BAYSAL ÜNİVERSİTESİ  
FEN BİLİMLERİ ENSTİTÜSÜ  
FİZİK ANABİLİM DALI  
(TEZ DANIŞMANI: PROF. DR. İBRAHİM BELENLİ)**

**BOLU, AĞUSTOS 2019**

$MgB_2$ , süper iletken özelliği yalnızca 2001 yılında keşfedilmesine rağmen neredeyse on yıllardan beri bilinmektedir. O zamandan beri, süper iletken kablolar, bobinler ve mıknatıslar, kolaylık ve uygun maliyetli kullanılabilirliği nedeniyle oldukça yaygın hale gelmiştir.  $MgB_2$ , düşük sıcaklık (LT) süper iletkenleri (örneğin NbTi, 9K) ile düşük sıcaklık (LT) süper iletkenleri (örneğin NbTi, 9K) ve yüksek sıcaklık BSCCO (Bismuth stronsiyum kalsiyum bakır oksit) arasındaki ortadaki yer olan kritik bir sıcaklığa geldiğinde benzersiz bir süper iletkenidir. 108 K.

Süper iletkenlerin verimli çalışması için bu kritik sıcaklıklara ulaşması gerekir.  $MgB_2$ , önemli bir maliyet farkında kolayca bulunabilen sıvı hidrojen veya katı hal nitrojen / kriyo soğutucu kullanımıyla kolayca soğutulabilir.

Bu çalışmada,  $MgB_2$ 'nin süper iletkenlik özelliklerini, toplam karbon içeriklerinin % 3/6/9'u arasında değişen ve karbon içerikli farklı karbon içeren kaynaklarla (şeker ve malik asit) katkılanarak, kritik akım yoğunluğunu ve sıcaklığını geliştirmeyi amaçladık. Ön deneylerde, termogravimetrik koşullar (DTG, Ar) altında malik asit ve şeker ayrıştırıldı ve ağırlık değişiklikleri, ayrışma sıcaklığı ve saf karbon oluşumu (yaklaşık 400 ° C) belirlendi. Mg'nin bu aşamada eklenmesi, öncül malik asit ve şekerin ayrışması sırasında oluşan suyun varlığından dolayı uygun olmadı. Numunelerin faz saflığı, X-Ray difraksiyon yöntemi ile analiz edildi. Her bir örnekte hücre sabitlerinin (lattice constant) belirlenmesi için Rietveld analizi yapılmıştır. XRD'den sayısal bir terkip elde etmek için ölçülen yansımalar Si standardı eklenerek kalibre edildi. Sonuçlar, hücre parametrelerinde a ve c eksenlerinde saf  $MgB_2$ 'ye göre beklenen kaymaları göstermektedir. Çok tipik olarak, katkılı örnekteki  $MgB_2$ 'nin hücrelerinde C yerleştirme miktarıyla orantılı olarak c / a oranının artmasıdır. Aynı nominal karbon içeriklerinden başlayarak, şekerle doping, malik asidin C katkılayıcı olarak kullanılmasından daha etkilidir. Bunun, genel süreçte reaktanların ve özellikle de karbonun homojenliği ile doğrudan ilgili olduğuna inanıyoruz.

**ANAHTAR KELİMELER:**  $MgB_2$ , Malik Asit, Kritik Sıcaklık, Süperiletken, Reitveld Analizi, Örgü parametresi

# TABLE OF CONTENTS

	<u>Page</u>
<b>ABSTRACT</b> .....	<b>v</b>
<b>ÖZET</b> .....	<b>vi</b>
<b>TABLE OF CONTENTS</b> .....	<b>vii</b>
<b>LIST OF FIGURES</b> .....	<b>viii</b>
<b>LIST OF ABBREVIATIONS AND SYMBOLS</b> .....	<b>x</b>
<b>1. INTRODUCTION</b> .....	<b>1</b>
1.1 Magnesium Diboride .....	3
1.2 Properties of MgB <sub>2</sub> .....	4
1.3 Structure of Applied Superconductors .....	6
1.4 Production of MgB <sub>2</sub> Conductors .....	10
1.4.1 Carbon Addition .....	12
1.4.2 Powder Processing.....	13
1.4.3 Carbon doping on MgB <sub>2</sub> and Its Effects .....	14
<b>2. AIM AND SCOPE OF THE STUDY</b> .....	<b>18</b>
<b>3. MATERIALS AND METHODS</b> .....	<b>19</b>
3.1 Synthesis of Carbon Doped Boron powder .....	19
3.2 General Synthesis of C Doped Boron with Sugar and Malic Acid ....	20
<b>4. RESULT AND DISCUSSION</b> .....	<b>22</b>
<b>5. CONCLUSION AND RECOMMEDATIONS</b> .....	<b>31</b>
<b>6. REFERENCES</b> .....	<b>32</b>
<b>7. APPENDICES</b> .....	<b>36</b>
<b>8. CURRICULUM VITAE</b> .....	<b>46</b>



## LIST OF FIGURES

	<u>Page</u>
<b>Figure 1.1.</b> Graph of world helium extraction.(L. David Roper “Helium Depletion,” 2016) .....	1
<b>Figure 1.2</b> Crystal structure of MgB <sub>2</sub> (Silva-Guillén et al., 2015) .....	3
<b>Figure 1.3.</b> Critical surface and their use on conventional applications. ....	5
<b>Figure 1.4.</b> Superconductive wire which is formed by comb .....	7
<b>Figure 1.5.</b> Graph of superconductors by year and their cooling agents.....	8
<b>Figure 1.6.</b> Yield strength of the NbTi/Cu composite wire (Guan et al., 2015) 8	8
<b>Figure 1.7.</b> Stress-strain and its effect on Superconductors. ....	9
<b>Figure 1.8.</b> Method of production of powder in tube fabrication.....	11
<b>Figure 1.9.</b> Thermal treatment of MgB <sub>2</sub> .....	11
<b>Figure 1.10.</b> Depiction of ball-milling process of any solid state material. ....	13
<b>Figure 1.11.</b> TEM image of sample doped with 10% sugar.....	15
<b>Figure 1.12.</b> TEM image of pure MgB <sub>2</sub> sample. (Zhou et al., 2007) .....	15
<b>Figure 1.13.</b> Crystal structure of MgB <sub>2</sub> C <sub>2</sub> (Sawada et al., 2018) .....	17
<b>Figure 3.14.</b> Picture of cylindrical furnace.....	20
<b>Figure 3.15.</b> Diagram of MgB <sub>2</sub> Test and Production Appliances .....	21
<b>Figure 4.16.</b> TGA Graph of Commercial Sugar. (“Thermal Decomposition of Sucrose in Nitrogen Atmosphere   Lamentations on Chemistry,” 2008) .....	22
<b>Figure 4.17.</b> TGA Graph of Malic Acid.....	23
<b>Figure 4.18.</b> XRD diagrams of all C-doped MgB <sub>2</sub> powders. ....	23
<b>Figure 4.19.</b> XRD of 6% sugar carbon doped MgB <sub>2</sub> .....	24
<b>Figure 4.20.</b> Comparison of the XRD patterns of MgB <sub>2</sub> .....	24
<b>Figure 4.21.</b> Miller indices for MgB <sub>2</sub> .....	26
<b>Figure 4.22.</b> The lattice parameters of carbon (sugar) doping of MgB <sub>2</sub> .....	28
<b>Figure 4.23.</b> The malic acid assisted version of the C doping method .....	29
<b>Figure 7.24.</b> XRD of sample no:1 3% carbon doped (Sugar) MgB <sub>2</sub> .....	36
<b>Figure 7.25.</b> Rietveld analysis of 3% carbon (Sugar) doped MgB <sub>2</sub> .....	36
<b>Figure 7.26.</b> XRD of sample no:2 6% carbon doped (Sugar) MgB <sub>2</sub> sample. ..	38
<b>Figure 7.27.</b> Rietveld analysis of 6% carbon doped (Sugar) MgB <sub>2</sub> sample.....	38
<b>Figure 7.28.</b> XRD of sample no:3 9% carbon doped MgB <sub>2</sub> (Sugar) sample. ..	40
<b>Figure 7.29.</b> Rietveld analysis of 9% carbon doped (Sugar) MgB <sub>2</sub> .....	40
<b>Figure 7.30.</b> XRD of sample no:4 3% carbon doped with malic acid.....	42
<b>Figure 7.31.</b> Rietveld analysis of 3% carbon doped (Malic Acid) MgB <sub>2</sub> .....	42
<b>Figure 7.32.</b> 6% carbon doped with malic acid addition MgB <sub>2</sub> sample.....	44
<b>Figure 7.33.</b> Rietveld analysis of 6% carbon doped (Malic Acid) MgB <sub>2</sub> .....	44

## LIST OF TABLES

	<u>Page</u>
<b>Table 1.1.</b> List of some known superconductors and their corresponding critical temperature values. ....	2
<b>Table 1.2</b> $T_c$ value of $MgB_2$ and other superconductors.....	4
<b>Table 1.3.</b> Transition temperatures of some High- $T_c$ superconductors. (A. Augustyn, 2019) .....	5
<b>Table 1.4.</b> A collation of thermal stabilities superconductors .....	7
<b>Table 1.5.</b> Decomposition temperature of few aromatic hydrocarbons (Troyanov et al., 2002).....	16
<b>Table 3.6.</b> Specification of the mixing of carbon content with boron.....	19
<b>Table 4.7.</b> Carbon doping with sugar of $MgB_2$ and yield in grams. ....	25
<b>Table 4.8.</b> Carbon doping with DL-Malic acid of $MgB_2$ and yield. ....	25
<b>Table 4.9.</b> a and c lattice parameters of substances. ....	27
<b>Table 7.10.</b> Rietveld analysis of 3% carbon doped (Sugar) $MgB_2$ .....	37
<b>Table 7.11.</b> Lattice parameters calculated from (Klug & Alexander, 1974) ....	37
<b>Table 7.12.</b> Result from LECO Carbon analyzer 3% carbon doped (Sugar) ...	37
<b>Table 7.13.</b> Rietveld analysis of 6% carbon doped (Sugar) $MgB_2$ .....	39
<b>Table 7.14.</b> Lattice parameters calculated from (Klug & Alexander, 1974) ....	39
<b>Table 7.15.</b> Result from LECO Carbon analyzer 6% carbon doped (Sugar) ...	39
<b>Table 7.16.</b> Rietveld analysis of 9% carbon doped (Sugar) $MgB_2$ .....	41
<b>Table 7.17.</b> Lattice parameters calculated from (Klug & Alexander, 1974) ....	41
<b>Table 7.18.</b> Result from LECO Carbon analyzer 9% carbon doped (Sugar) ..	41
<b>Table 7.19.</b> Rietveld analysis of 3% carbon doped $MgB_2$ (Malic Acid).....	43
<b>Table 7.20.</b> Lattice parameters calculated from (Klug & Alexander, 1974) ....	43
<b>Table 7.21.</b> Result from Carbon analyzer 3% carbon doped Malic Acid .....	43
<b>Table 7.22.</b> Rietveld analysis of 6% carbon doped $MgB_2$ (Malic Acid) .....	45
<b>Table 7.23.</b> Lattice parameters calculated from (Klug & Alexander, 1974) ....	45
<b>Table 7.24.</b> Result from Carbon analyzer 6% carbon doped Malic Acid .....	45

## LIST OF ABBREVIATIONS AND SYMBOLS

<b>BCS</b>	: Bardeen–Cooper–Schrieffer theory
<b><math>J_c</math></b>	: Critical Current Density
<b>K</b>	: Kelvin
<b>MgB<sub>2</sub></b>	: Magnesium Diboride
<b>MgO</b>	: Magnesium Oxide
<b>MRI</b>	: Magnetic Resonance Imaging
<b>Nb-Ti</b>	: Niobium Titanium
<b>Si</b>	: Silicon
<b>T</b>	: Tesla
<b><math>T_c</math></b>	: Critical Temperature
<b>TEM</b>	: Transmission Electron Microscopy
<b>TGA</b>	: Thermogravimetric Analysis
<b>XRD</b>	: X-Ray Diffraction
<b>kV</b>	: Kilovolt
<b>mA</b>	: Milliampere
<b>Nb Sn</b>	: Niobium-Tin
<b>NbTi/Cu</b>	: Niobium – Titan
<b>MRI</b>	: Magnetic Resonance Imaging
<b>ITER</b>	: International Thermonuclear Experimental Reactor
<b>HEP</b>	: High Energy Physics
<b>NMR</b>	: Nuclear Magnetic Resonance

## **ACKNOWLEDGEMENTS**

I wish to express my deepest gratitude to my supervisor Prof. Dr. İbrahim BELENLİ for his guidance, advice, criticism, encouragements and insight throughout the research.

I would also like to thank Assoc. Prof. Dr. Mehmet SOMER for his suggestions and comments.

## 1. INTRODUCTION

In this thesis we have aimed to improve methods used for synthesis of carbon doped  $\text{MgB}_2$ .  $\text{MgB}_2$  itself is a great superconductor because of its high  $T_c$ . This enables it to be cooled with liquid hydrogen or using combined solid nitrogen-cryo-cooler, while the most Type-I superconductors require liquid helium environment to be cryo-cooled. Another problem with the coolant and  $T_c$  is the helium reserves of earth. Very few natural gas wells in the world have enough helium to separate it economically from natural gas. The gas wells with the most helium content do not exceed 3% percent, so it is in short supply. (Kornbluth, 2019)

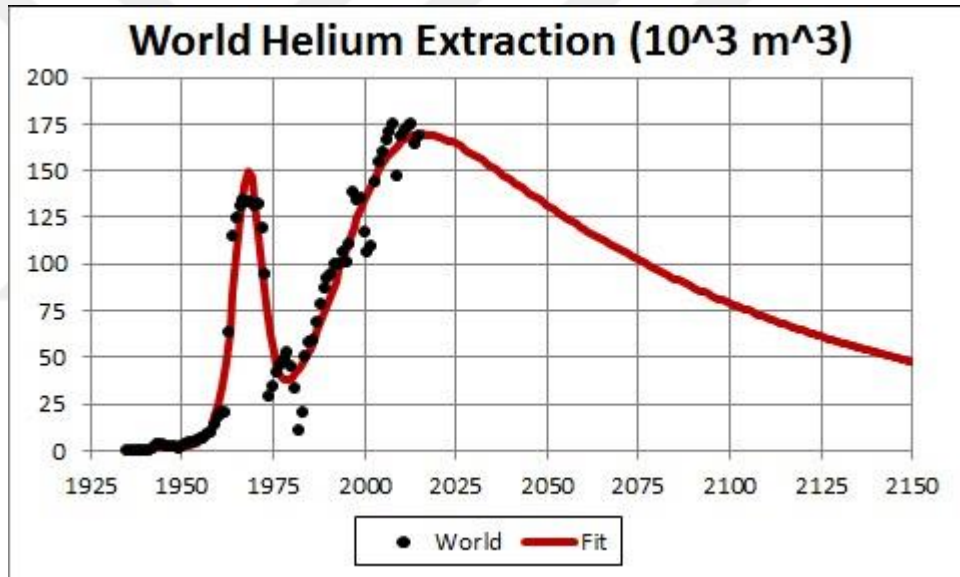


**Figure 1.1.** Graph of world helium extraction (L. David Roper, 2016).

While world helium reserves are diminishing, need for reducing helium usage initiated new developments in cryo-coolers. Use of solid nitrogen opened a new area for cooling method. Temperature is lowered down to 10K with a cryo-cooler and meanwhile the superconductor is submerged in solidified nitrogen. The only downside of this application is the cooling time of the liquid nitrogen bed (77K) into solid nitrogen using a cooling power of 6 W at 10 K and 15 W at 15 K which may take 5 to 7 days. (Yao et al., 2008)

With  $T_c = 39\text{K}$ ,  $\text{MgB}_2$  is the perfect candidate for this operation due to its availability and low upkeep costs compared to other superconductors that require liquid helium to operate (Table 1.1)

**Table 1.1.** List of some known superconductors and their corresponding critical temperature values.

<b>Compound</b>	<b><math>T_c</math> (K)</b>	<b>Compound</b>	<b><math>T_c</math> (K)</b>
<b><math>\text{Ba}_8\text{Si}_{46}</math></b>	8.07	<b><math>\text{C}_{60}\text{Rb}_x</math></b>	28
<b><math>\text{C}_6\text{Ca}</math></b>	11.5	<b><math>\text{FeB}_4</math></b>	2.9
<b><math>\text{C}_6\text{Li}_3\text{Ca}_2</math></b>	11.15	<b><math>\text{InN}</math></b>	3
<b><math>\text{C}_8\text{K}</math></b>	0.14	<b><math>\text{In}_2\text{O}_3</math></b>	3.3
<b><math>\text{C}_8\text{KHg}</math></b>	1.4	<b><math>\text{LaB}_6</math></b>	0.45
<b><math>\text{C}_6\text{K}</math></b>	1.5	<b><math>\text{MgB}_2</math></b>	39
<b><math>\text{C}_3\text{K}</math></b>	3.0	<b><math>\text{Nb}_3\text{Al}</math></b>	18
<b><math>\text{C}_3\text{Li}</math></b>	<0.35	<b><math>\text{Nb}_3\text{Ge}</math></b>	23.2
<b><math>\text{C}_2\text{Li}</math></b>	1.9	<b><math>\text{NbO}</math></b>	1.38
<b><math>\text{C}_3\text{Na}</math></b>	2.3–3.8	<b><math>\text{NbN}</math></b>	16
<b><math>\text{C}_2\text{Na}</math></b>	5.0	<b><math>\text{Nb}_3\text{Sn}</math></b>	18.3
<b><math>\text{C}_8\text{Rb}</math></b>	0.025	<b><math>\text{NbTi}</math></b>	10
<b><math>\text{C}_6\text{Sr}</math></b>	1.65	<b><math>\text{SiC:B}</math></b>	1.4
<b><math>\text{C}_6\text{Yb}</math></b>	6.5	<b><math>\text{SiC:Al}</math></b>	1.5
<b><math>\text{C}_{60}\text{Cs}_2\text{Rb}</math></b>	33	<b><math>\text{TiN}</math></b>	5.6
<b><math>\text{C}_{60}\text{K}_3</math></b>	19.8	<b><math>\text{ZrN}</math></b>	10

On the Table 1.1 as it can be seen that  $\text{MgB}_2$ 's critical temperature is at the range of liquid hydrogen coolant, which makes it a lot cheaper to operate than its peers shown above.

## 1.1 Magnesium Diboride

Magnesium diboride was discovered around late 50's but its superconductive properties did not acknowledged up until early 2000's (High & Field, 2001).

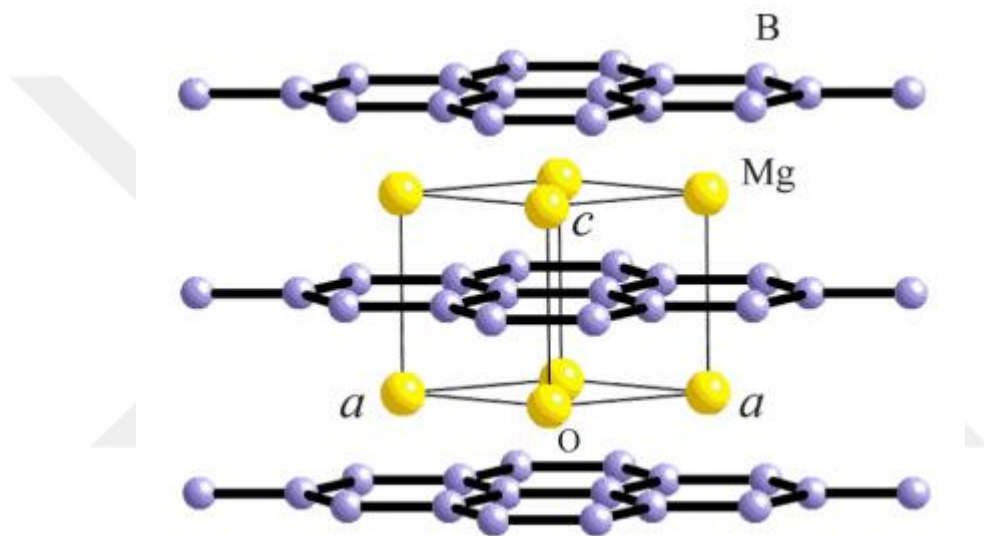


**Figure 1.2** Crystal structure of  $\text{MgB}_2$  (Silva-Guillén et al., 2015)

$\text{MgB}_2$  has a higher  $T_c$  than its previous metallic versions of superconductors, such as NbTi,  $\text{Nb}_3\text{Sn}$  etc. revealing two-gap superconductivity (Buzea & Yamashita, 2001). Which means it has two superconducting gaps with different sizes on different disconnected parts of its Fermi surface.

What makes magnesium diboride an appealing is that, it can be easily operated below 39 K (especially around 20 K) which can be achieved with relative ease by conventional methods. In contrast to other high  $T_c$  conductors,  $\text{MgB}_2$  became more popular due to its simple composition and ease of synthesis from the starting elements. The price of its components are cheaper than those of the other LT and HT than other conductors, its simple production makes its performance/cost ratio to be

around 50 to 200 times higher than any other high  $T_c$  superconductor (Cooley, Ghosh, & Scanlan, 2005).

**Table 1.2**  $T_c$  value of MgB<sub>2</sub> and other superconductors

Material	$T_c$ (K)	$\Delta$ (meV)	$\xi_{GL}$ (nm)	$\lambda_L$ (nm)	$B_c, B_{c2}$ (T)
Pb	7.2	1.38	51–83	32–39	0.08 ( $B_c$ )
Nb	9.2	1.45	40	32–44	0.2 ( $B_c$ )
NbN	13–16	2.4–3.2	4	250	16
Nb <sub>3</sub> Sn	18	3.3	4	80	24
Nb <sub>3</sub> Ge	23.2	3.9–4.2	3–4	80	38
NbTi	9.6	1.1–1.4	4	60	16
YBa <sub>2</sub> Cu <sub>3</sub> O <sub>7</sub>	92	15–25	1.6 ( <i>ab</i> )	150 ( <i>ab</i> )	240 ( <i>ab</i> )
Bi <sub>2</sub> Sr <sub>2</sub> CaCu <sub>2</sub> O <sub>8</sub>	94	( <i>max., ab</i> )	0.3 ( <i>c</i> )	800 ( <i>c</i> )	110 ( <i>c</i> )
		15–25	2 ( <i>ab</i> )	200–300 ( <i>ab</i> )	>60 ( <i>ab</i> )
Bi <sub>2</sub> Sr <sub>2</sub> Ca <sub>2</sub> Cu <sub>3</sub> O <sub>10</sub>	110	( <i>max., ab</i> )	0.1 ( <i>c</i> )	>15 000 ( <i>c</i> )	>250 ( <i>c</i> )
		25–35	2.9 ( <i>ab</i> )	150 ( <i>ab</i> )	40 ( <i>ab</i> )
MgB <sub>2</sub>	40	1.8–7.5	10 ( <i>ab</i> )	110 ( <i>ab</i> )	15–20 ( <i>ab</i> )
			2 ( <i>c</i> )	280 ( <i>c</i> )	3 ( <i>c</i> )
Ba <sub>0.6</sub> K <sub>0.4</sub> Fe <sub>2</sub> As <sub>3</sub>	38	4–12	1.5 ( <i>ab</i> )	190 ( <i>ab</i> )	70–235 ( <i>ab</i> )
			$c > 5$ ( <i>c</i> )	0.9 ( <i>c</i> )	100–140 ( <i>c</i> )
NdO <sub>0.82</sub> F <sub>0.18</sub> FeAs	50	37	3.7 ( <i>ab</i> )	190 ( <i>ab</i> ) <i>c</i>	62–70 ( <i>ab</i> )
			0.9 ( <i>c</i> )	>6000 ( <i>c</i> )	300 ( <i>c</i> )

Above table 1.2 shows the  $T_c$  value of MgB<sub>2</sub> and other superconductors and also their london penetration depth  $\lambda_L$  and their critical magnetic field  $B_c$  (Alecu, Stancu, Zamfir, & Cosac, 2007).

## 1.2 Properties of MgB<sub>2</sub>

Superconductors in magnet systems drastically reduce the power consumption rate but it also affected by critical surface of the material that is being made. High  $T_c$  superconductors are always preferred for electromagnets applications for performing at 77 K.



**Table 1.3.** Transition temperatures of some High- $T_c$  superconductors. (A. Augustyn, 2019)

Transition Temperatures of Some High- $T_c$ Superconductors	
compound	$T_c$ (K)
$\text{Nd}_{1.85}\text{Ce}_{0.15}\text{CuO}_4$	24
$\text{La}_{1.85}\text{Sr}_{0.15}\text{CuO}_4$	40
$\text{YBa}_2\text{Cu}_3\text{O}_7$	92
$\text{Bi}_2\text{Sr}_2\text{Ca}_2\text{Cu}_3\text{O}_{10}$	110
$\text{Tl}_2\text{Ba}_2\text{Ca}_2\text{Cu}_3\text{O}_{10}$	127
$\text{Hg}_2\text{Ba}_2\text{Ca}_2\text{Cu}_3\text{O}_8$	134

Nowadays, the vast majority of superconductor magnets are made out of Nb-Ti wires or its combination. Reason for that is NbTi wires can carry supercurrent up to 5 T at around 4.2K. (Larbalestier, 1980)

Considering the commercial use of superconducting electromagnets, both Nb-Ti and  $\text{MgB}_2$  have similarities since magnetic field dependence of their transport behaviors are similar.

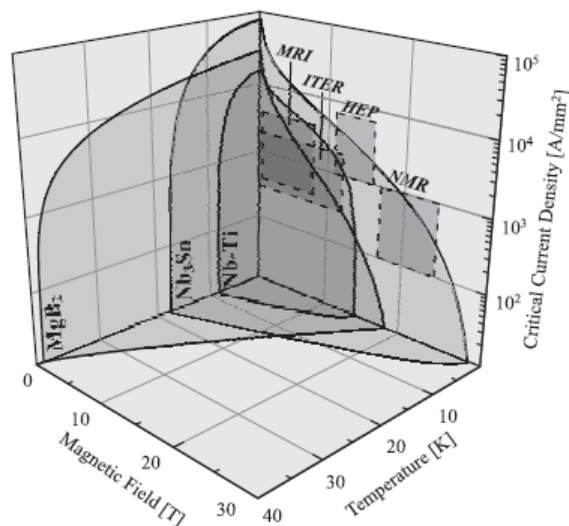


**Figure 1.3.** Critical surface and their use on conventional applications.

The high  $T_c$  of  $MgB_2$  magnets allows them to be used in high temperature applications, also  $J_c$  performance ratio of  $MgB_2$  conductors can have a high magnetic fields at 8 Tesla operating temperature around low temperatures around 18 to 20K. (Vajpayee et al., 2008 n.d.)

Since this temperature can be relatively easily reached and these magnets are significantly better in terms of cost/efficiency, there is no need of using a liquid helium cryostat to cool the conductor.

Temperature of 20K can be easily reached with solid nitrogen or  $H_2$  which can be used as a cryogenic liquid (Larminie & Dicks, 2003). Although it looks convenient to use liquid hydrogen, it has some flaws as well;

- Low gas density, the size of a gasoline tank is three times less the amount compared to a liquid hydrogen tank. (“The Advantages and Disadvantages of Liquid Hydrogen - Liquid Hydrogen vs. Fossil Fuels,” 2018)
- High specific heat
- High thermal conductivity: The value of thermal conductivity for most gases and vapors range between 0.01 and 0.03 W/mK at room temperature while that of hydrogen gas is 0.18 W/mK. (“The thermal conductivity of gases | Electronics Cooling,” 1998.)

### **1.3 Structure of Applied Superconductors**

The application of conventional superconductors illustrated by their stable and easy to use operation. Superconductors are made having various number of superconducting filaments which are placed in highly conductive matrixes as show in figure 1.4.

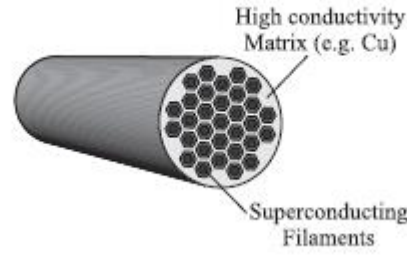


**Figure 1.4.** Superconductive wire which is formed by comb

It is an important factor for a superconductor to carry a high current density without any losses during the transfer of current due to thermal loss. It is possible to release a small amount of heat during the transfer of current even for superconductors which results in increasing temperature of the material locally above its  $T_c$  (Kovalenko, 2017). These temperature increases could eventually cause a hot-spot at which heat would accumulate overtime, and this hot spot can cause a local increase of temperature on the magnet and evidently melt down the wire if the accumulated heat is not equally drained while generated.

Wire itself has to turn back to normal zone which is inversely proportional to its minimum quench energy. This is determined by few factors which; volumetric heat capacity, heat generation, and thermal conductivity for heat drainage. Also it is affected by heat propagation speed along the wire. A faster propagating heat means it is quick spreading along the wire which makes wire to stay on its local temperature.

**Table 1.4.** A collation of thermal stabilities superconductors

		Nb <sub>3</sub> Sn		MgB <sub>2</sub>		Bi <sub>2</sub> Sr <sub>2</sub> Ca <sub>2</sub> Cu <sub>3</sub> O <sub>x</sub>
		$T = 4.2$ K	$T = 4.2$ K	$T = 20$ K	$T = 77$ K	
Matrix		Cu	Cu (Fe) <sup>b</sup>		Ag	
$f$	[%]	55	55 <sup>c</sup>		30	
$B^a$	[T]	10	3		0	
$T_c(B)^a$	[K]	13	35		110	
$J_c(B)^a$	[·100A/mm <sup>2</sup> ]	40	20	6	2	
$\kappa^a$	[W/mK]	384	173 (3)	691 (35)	436	
$\rho^a$	[·10 <sup>-9</sup> Ωm]	0.3	0.6 (15)	0.6 (14)	5	
$c^a$	[·10 <sup>3</sup> J/m <sup>3</sup> K]	1.2	0.7 (1.7)	34 (20)	1550	
$D_T$	[·10 <sup>-3</sup> m <sup>2</sup> /s]	329	243 (1.5)	21 (1.7)	0.3	
MQE	[·10 <sup>-3</sup> J]	0.1	3.3 (0.04)	90 (0.14)	611	

Minimum quench energy and normal zone depending on matrix materials as can be seen from figure above. Higher the conducting matrix results in heat drainage

faster. Normal zone is hard to detect due to its slow expansion rate. At operating temperature of 4.2K Nb<sub>3</sub>Sn and MgB<sub>2</sub> have a lot of similarities, but MgB<sub>2</sub> can function up to 20K in terms of suitability.

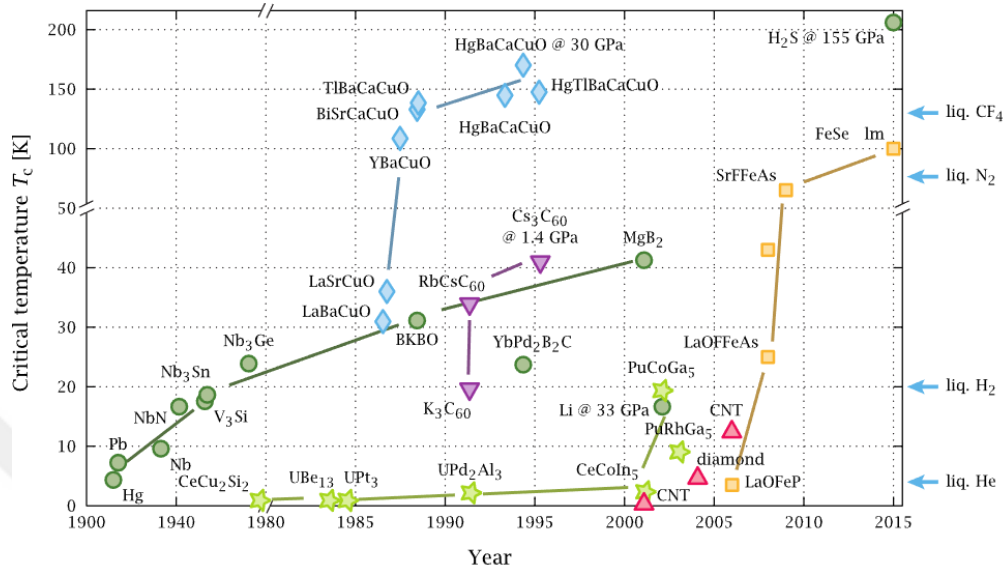


**Figure 1.5.** Graph of superconductors by year and their cooling agents

In addition to thermal stability, mechanical stress response may also impose strict boundary conditions in a practical superconductor design.

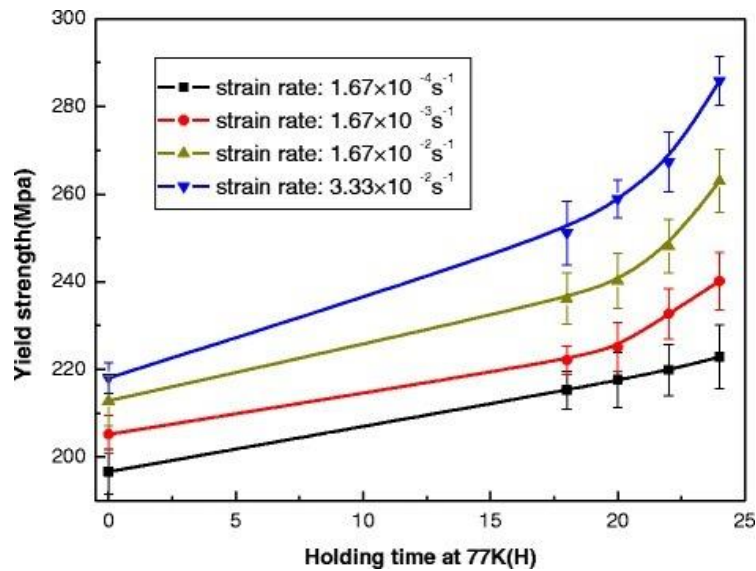


**Figure 1.6.** Yield strength of the NbTi/Cu composite wire (Guan et al., 2015)

At low stress level superconducting properties show a reduction in  $T_c$  when the pressure is increased (Müller & Saur, 1964).

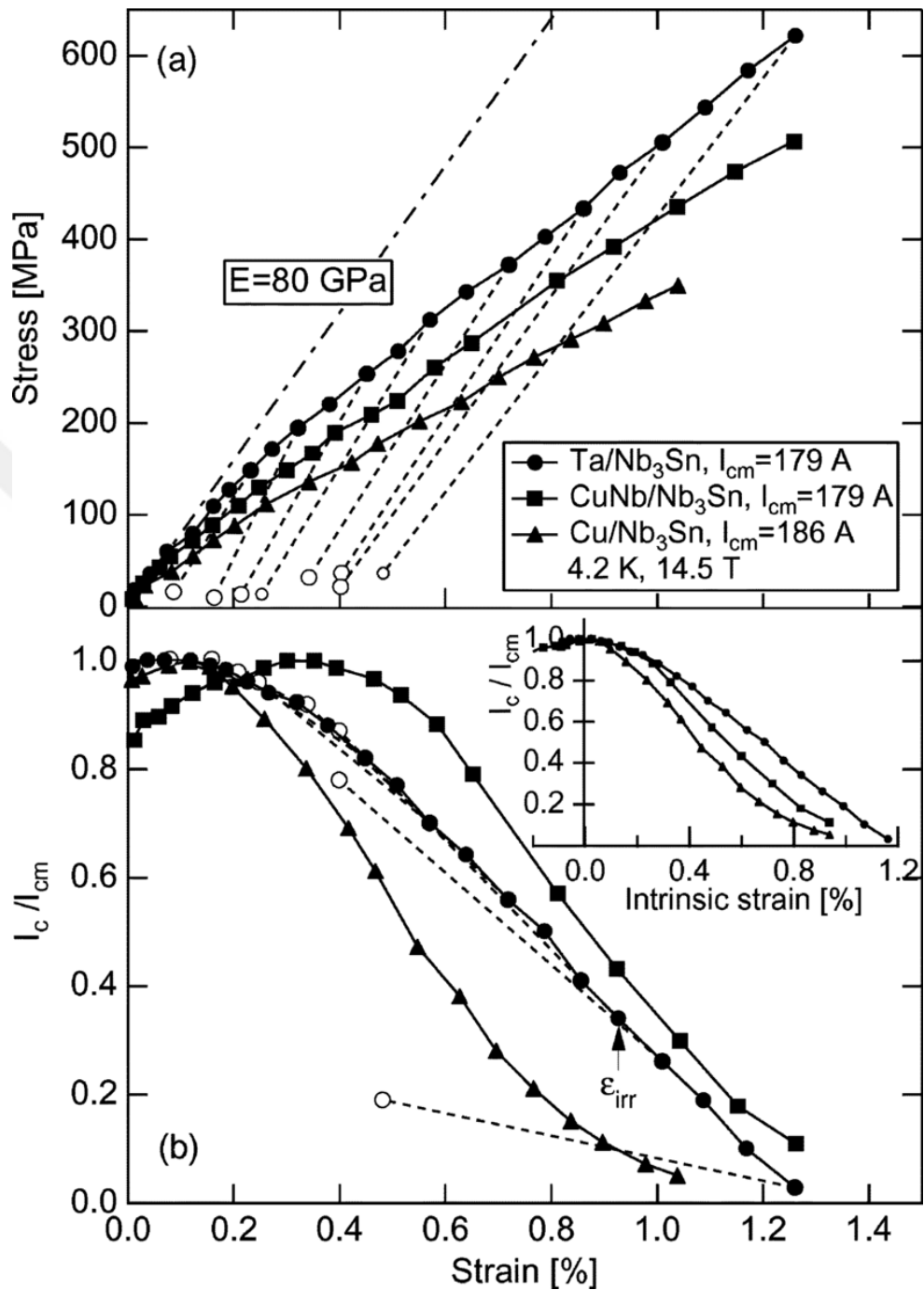


**Figure 1.7.** Stress-strain and its effect on Superconductors.

(a) Stress-strain characteristics of high-strength Nb Sn superconductors. The strength of Ta=Nb Sn wire was much higher than not only that of conventional

Cu=Nb Sn but also high-strength CuNb=Nb Sn wires. (b) Normalized critical current as a function of tensile strain (Nishijima et al., 2005).

Even though, the effect of hydrostatic pressure on superconductors known for a long time it took some time to characterize the superconductors by their mechanical strain. Strain in applied superconductors by thermal strain built up in a composite superconductor after its cooled down from its heat treatment phase to its operating temperature, due to difference between thermal contraction of its filament and matrix. Then, its subjugation to wire when conductor is subjected to a large bending and torsion when its first bundled up into a cable and wound into a coil. Lastly, and the most importantly the stress build up due to Lorentz force generated by high current and high magnetic field.

Although there is limited amount of research in terms of  $MgB_2$  in regards to mechanical and thermal strain, these subjects are an important study for further scientific findings.

#### **1.4 Production of $MgB_2$ Conductors**

Conventional conductors are made of thin films of superconducting material placed on to conducting matrixes. Wires are adjusted to the desired sizes by drawing or pressing. While for some superconductors its easy to do these processes,  $MgB_2$  is hard to follow up due to its intermetallic compound structure.

Since this diffusion technique is not conventional to be used, putting powder inside a tube became the regular the production method of the  $MgB_2$  wire.

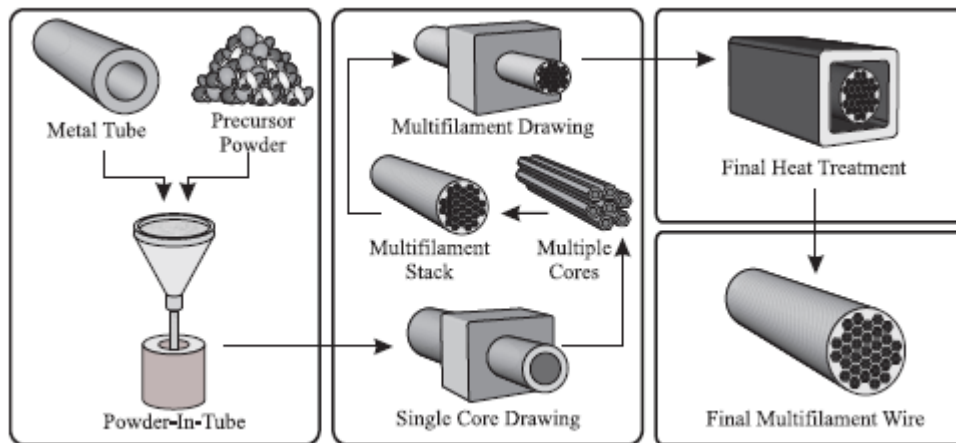


**Figure 1.8.** Method of production of powder in tube fabrication

The tube in which powder resides in a part of the matrix at the end so it has to be both electrically and thermally highly conductive.  $MgB_2$  reacts with a lot of known elements such as copper or aluminium which makes it hard to decide what tube that has to be used. Materials that are relatively chemically stable for  $MgB_2$  are steel, iron or nickel. Although these materials are hard and not good at electrical and thermal conductivity, they are stable enough to be used without having any diffusion deformations with less chemical incompatibility in the form of diffusion of B. (Tolga & Ibrahim, 2016)

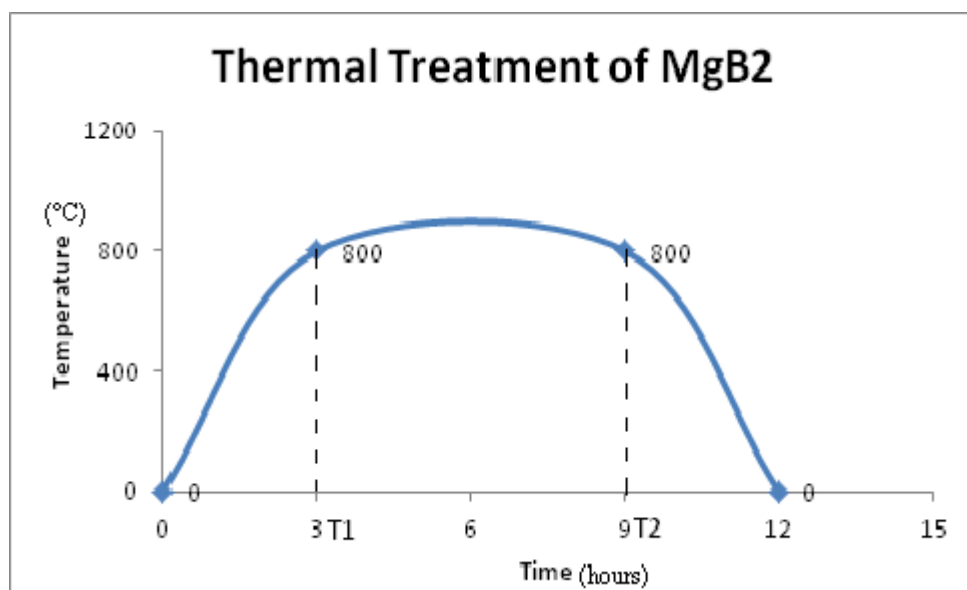


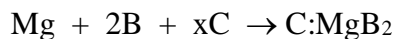
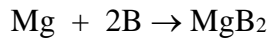
**Figure 1.9.** Thermal treatment of  $MgB_2$

Thermal treatment of MgB<sub>2</sub> superconductor during its production, T<sub>1</sub> and T<sub>2</sub> signifies the ramp, heating and cooling temperatures accordingly.

### 1.4.1 Carbon Addition

After its discovery, MgB<sub>2</sub> conductors became popular among the conventional superconductors due to their easier fabrication process and higher operation temperature which does not require liquid-helium-free coolants. Second impact has been made after realizing that it can also be significantly enhanced by addition of carbon based compounds. This enhancement is expressed by the increase of the critical current density  $J_c$  as a function of applied magnetic field (Zhou, Pan, Wexler, & Dou, 2007).

Almost 20 years of extensive research efforts gave rise to noticeable progress in MgB<sub>2</sub> wire fabrication showing superior high field properties with respect to other superconductors. However, the low field performance could not be improved in the same measure. Indeed,  $J_c$  is even lower than the other conductors below 5 T which has been associated to lack of permeable nature of the material.



Chemical reaction formula above shows the production of MgB<sub>2</sub> doped with C of our choice in equation.

Carbon doping to MgB<sub>2</sub> is not a straight forward process. There are different techniques which have their advantages and disadvantages. The simplest one is the mixing and reacting of the solid components Mg, B and graphite which unfortunately yields non-homogenous products. Better results were achieved when hydrocarbons instead of pure carbon was employed. Most widely used one is DL-Malic acid. Due to its soluble nature, low melting point and simple structure, it has an advantage over other direct carbon dopants such as graphite, graphene etc. Homogeneity acquired by using hydrocarbons resulting in a high  $J_c$  value matched with nanoparticles of SiC (Li & Dou, 2010)



### 1.4.2 Powder Processing

Ball-milling has been frequently employed to produce fine  $\text{MgB}_2$  (Xu et al., 2006).

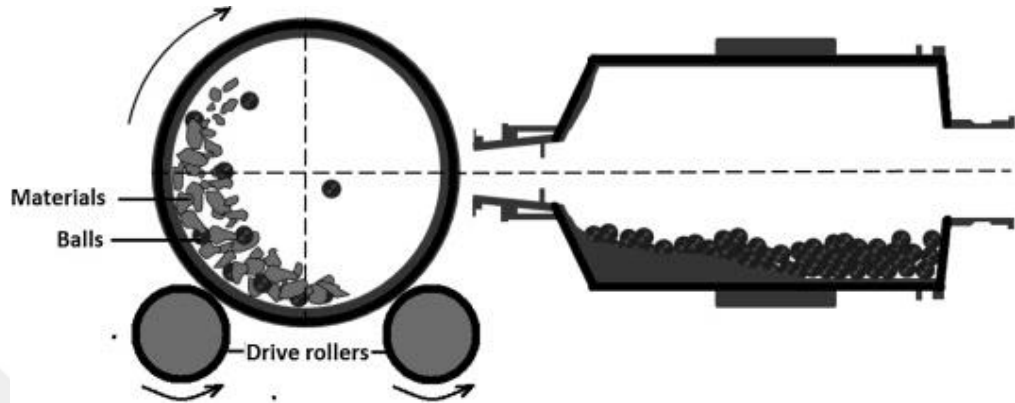


**Figure 1.10.** Depiction of ball-milling process of any solid state material.

Since  $\text{MgB}_2$  is a relatively hard material, particle size distribution is an important issue (Loh, Samanta, & Sia Heng, 2014). Separately, improved connectivity which leads to higher  $J_c$  values, reducing the particle size can also lead to better field of retention of the critical current (Giunchi et al., 2004). Also confirmed is the contribution of the grain size to increase of the irreversibility field  $B$ , which can be associated to improved boundary pinning.

The ball-milling method is conventionally easy and applicable to almost every solid material when it comes to mixing. But there is a small problem regarding the compounds nature when it comes to mixing this way. The longer ball milled matter remain in the chamber, the more agglomeration occurs which affects the particle size in the end product. An important challenge is achieving homogeneity around a small amount of nano-additives and matrix materials, since dry mixing poses the major problem of nanoparticle agglomeration. (T. Arai, 2015 )

### 1.4.3 Carbon doping on MgB<sub>2</sub> and Its Effects

Since the discovery of MgB<sub>2</sub>, various dopants have been introduced to improve its properties and to enhance its superconducting performance. However, as discussed above there is a problem with homogeneity regarding small amount of nano-additives and matrix materials. Since homogeneity is a problem in dry mixing process due to nano particle agglomeration, we have tried improving the homogeneity by introducing most readily available carbohydrates into MgB<sub>2</sub> by liquid homogeneous doping, namely sugar. Sugar doping has turned out to be an effective substitution method for carbon and boron in MgB<sub>2</sub> so that a significant enhancement of  $J_c$  could be achieved over an applied range field (Zhou et al., 2007).

One major problem for pure MgB<sub>2</sub> is the presence of relatively weak pinning centers leading to a rapid deformation of  $J_c$  as a function of B. Chemical doping is a way to prevent or even strengthen the pinning centers. The method is easy, cheap and a suitable way to introduce pinning sites into a superconductor.

As afore mentioned, carbon is introduced into MgB<sub>2</sub> crystal lattice by replacement of boron which leads to a decrease of the anionic charge coupled with formation of additional Mg vacancies due to the requirement of the overall charge balance. Parallely, the substitution enhances the charge carrier scattering occurring on Carbon substituted sites in Mg vacancies (Bateni et al., 2015).

Generally, nanometer sized particles are needed to ensure a homogeneous doping procedure, but no matter how well mixing, grinding, milling is carried out doping process is always impeded by agglomeration of particles.

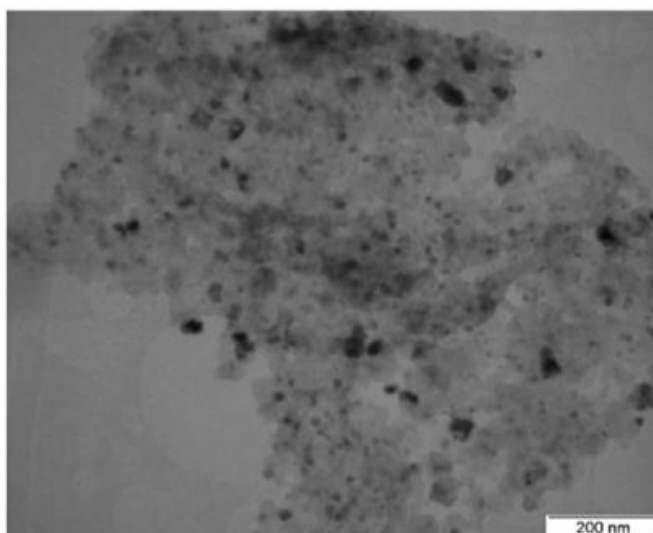


**Figure 1.11.** TEM image of sample doped with 10% sugar.

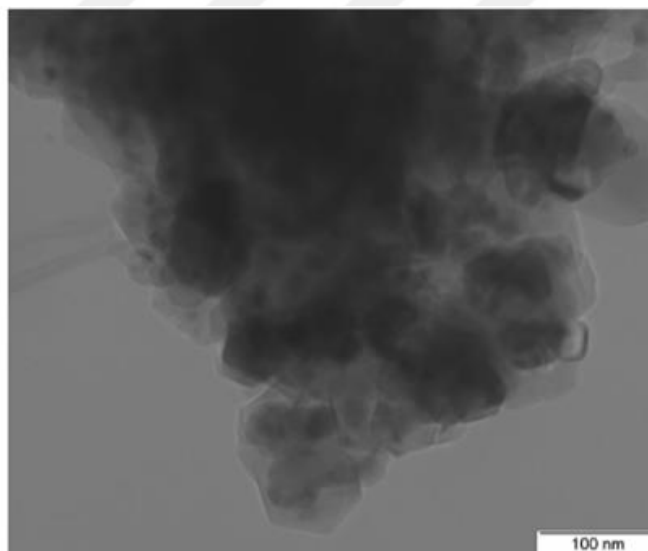


**Figure 1.12.** TEM image of pure MgB<sub>2</sub> sample. (Zhou et al., 2007)

TEM images show the impurities in sugar doped sample. Sugar doped contains more impurities are slightly bigger than undoped sample. The reduction of grain size is the result of impurity particles introduced by the doping which can serve as an additional nucleation site for grain formation.

Although, nano-size precursor particles were chosen for doping, it is a great challenge to reach homogeneity distribution of small amount of nano dopants within

the matrix materials through solid state mixing. Agglomeration has always been a problem on nano additive precursors.

Various forms of C have been attempted to introduce into boron but a remarkable success could not be achieved yet, due to its poor reactivity at the reaction temperature of MgB<sub>2</sub>. Also the use of carbon in form of hydrocarbons failed because of their high volatility already at moderate temperatures.

**Table 1.5.** Decomposition temperature of few aromatic hydrocarbons (Trojanov et al., 2002)

Adduct Composition	Decomposition Temperature, °C	$\Delta H_{dec}^a$ , kJ/mole	Solubility, mg/mL ( $\pm 0.04$ )
C <sub>60</sub> F <sub>18</sub> · 2C <sub>6</sub> H <sub>6</sub>	50–130	} 70(8) <sup>b</sup>	0.48
C <sub>60</sub> F <sub>18</sub> · C <sub>6</sub> H <sub>6</sub>	130–160		
C <sub>60</sub> F <sub>18</sub> · C <sub>6</sub> H <sub>5</sub> CH <sub>3</sub>	120–190	55(3)	0.52
C <sub>60</sub> F <sub>18</sub> · 2 <i>o</i> -C <sub>6</sub> H <sub>4</sub> (CH <sub>3</sub> ) <sub>2</sub>	40–80	61(6)	0.75
C <sub>60</sub> F <sub>18</sub> · <i>o</i> -C <sub>6</sub> H <sub>4</sub> (CH <sub>3</sub> ) <sub>2</sub>	110–180	55(5)	
C <sub>60</sub> F <sub>18</sub> · <i>m</i> -C <sub>6</sub> H <sub>4</sub> (CH <sub>3</sub> ) <sub>2</sub>	120–160	47(4)	1.23
C <sub>60</sub> F <sub>18</sub> · 2 <i>p</i> -C <sub>6</sub> H <sub>4</sub> (CH <sub>3</sub> ) <sub>2</sub>	50–100	38(4)	0.96
C <sub>60</sub> F <sub>18</sub> · <i>p</i> -C <sub>6</sub> H <sub>4</sub> (CH <sub>3</sub> ) <sub>2</sub>	100–160	31(4)	

To overcome such a problem, other hydrocarbon based materials were utilized as dopant, one of which is DL-malic acid (Bateni et al., 2015). There are several advantages of using hydrocarbons instead of pure carbon. Firstly, they can easily be dissolved in organic solvents forming slurry with boron which evidently increase its homogeneity. After evaporation of the solvent the obtained boron powder is uniformly coated with previously applied carbon material (Kim et al., 2006).

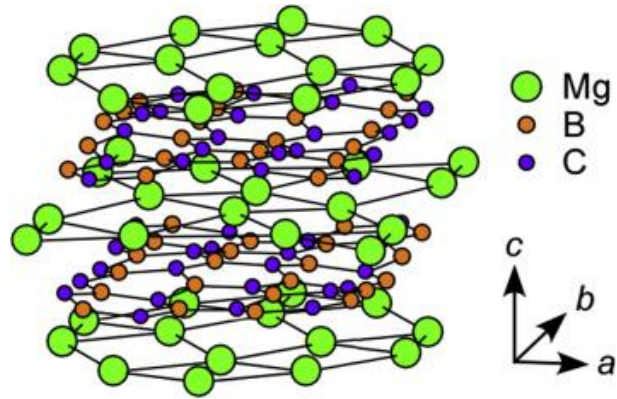


**Figure 1.13.** Crystal structure of MgB<sub>2</sub>C<sub>2</sub> (Sawada et al., 2018)

Secondly, hydrocarbons melt at lower temperature and decompose long below the formation temperature of MgB<sub>2</sub>. Therefore generation of a fresh layer of C on atomic scale reduces also the amount of carbon monoxide which may lead to formation of by products, such as MgB<sub>2</sub>C<sub>2</sub>. Lastly, due to the high reactivity of freshly formed carbon, the substitution of boron by carbon can take place at the same temperature as the formation MgB<sub>2</sub>.

The simultaneous reaction promotes C substitution for boron in the lattice and the inclusion of excess C within the grains resulting in enhancement of  $J_c$ . Although it results in small depression in  $T_c$ , carbohydrate substitution significantly increases the C substitution levels which results in diminishing of the impurity level and therefore improving the performance on all operating temperatures in the field range.

Carbohydrates like sugar, DL-malic acid are easily available and cheap. This procedure solves also the problem regarding agglomeration on nano sized particles and no longer need to use expensive nano additives while achieving high performance properties. Doping with them provides an efficient and desirable way to obtain homogeneous inexpensive and most importantly deformation free mixing.

## 2. AIM AND SCOPE OF THE STUDY

In this study the major part of the investigations is focused on the question which method and precursor compound is the most suitable one for the production of C doped MgB<sub>2</sub> powder to be used in superconducting wires.

For this purpose, we have synthesized MgB<sub>2</sub> with two carbohydrate containing precursors as dopant; DL-malic acid, and sugar. It is a well-known fact that a good amount of enhancements in electromagnetic properties in MgB<sub>2</sub> has been acquired through doping with various carbon forms. Doping effects are limited by agglomeration due to the mixing methods. For this purpose, Mg and boron (molar ratio 1:2) will be thoroughly blended with 3%, 6%, and 9% -wt of sugar or DL-malic acid, respectively. After the heat treatment, the results will be discussed analyzed in terms carbon content.

### 3. MATERIALS AND METHODS

Amorphous elemental Boron reagents were provided by Pavezyum Advanced Chemicals, Magnesium and malic acid were purchased from Sigma-Aldrich and Alfasol, respectively. Household sugar was used as second carbon source. Bruker D2 phaser – X-ray diffractometer and Bruker D8 – advanced X-Ray diffractometer was employed for the analysis of the educts and products in the 2theta range of 20°- 80° and at 40 kV and 15 mA with a variable rotation at 20 rpm along with 360° Phi. Slit width of 0.100mm and increment of 0.01160 were used. All measurements were performed with an increment of 1°/per minute in a total time of 60 minutes. The powder samples were mixed in a LORTONE tumbler for 1 hour for before the reaction for the heat treatment a vertical tube furnace was used equipped with a standard Cr-NiCr thermocouple. Carbon content (%-wt) of precursor's malic acid and sugar) has been analyzed by TGA (Thermogravimetric Analyzer) Q500 after the reaction.

#### 3.1 Synthesis of Carbon Doped Boron powder

The stoichiometric synthesis of  $MgB_2$  requires 0,47 / 0,53 mol ratio of B and Mg, but since pure carbon cannot be used for doping, the exact amount of the precursor sugar/malic acid has to be calculated separately beforehand. For this purpose, we used the thermogravimetric analysis method.

**Table 3.6.** Specification of the mixing of carbon content with boron

<b>C type</b>	<b>C ratio</b>	<b>Amount</b>
<b>Sugar</b>	3%	0,2g
	6%	0,4g
	9%	0,6g
<b>DL-Malic Acid</b>	3%	0,68
	6%	1,36

### 3.2 General Synthesis of C Doped Boron with Sugar and Malic Acid

Using the thermogravimetric analysis (TGA), one can easily calculate how much carbon is left after thermal decomposition of the precursor. This amount corresponds to the real carbon content to be accumulated in the  $\text{MgB}_2$  sample. We used a standard batch consisting of 0.94 g B along with 1.06 g Mg to be mixed with the required amount carbon source. It is important to note that this mixing cannot be accomplished straight forward, i.e.  $\text{Mg} + 2\text{B} + \text{carbon source}$ , since both precursors decompose at ca. 400 C to yield  $\text{H}_2\text{O}$ , CO and  $\text{CO}_2$  as gaseous products. Since Mg is very sensitive to water, air and CO, a major part of the magnesium would react with water vapor and air to form magnesium oxide and would be lost for the main reaction.



**Figure 3.14.** Picture of cylindrical furnace

Therefore, thermal decomposition of the precursor has to be done in presence of boron which results in formation thin layer of reactive, amorphous carbon coating onto boron powder. In the case of sugar addition, 0,94g B powder is placed inside a metallic tube together with the required amount of sugar (0,2 for 3%/ 0,4 for 6%/ 0,6 for 9%) which in turn was inserted in an outer silica tube in Fig.3.15.



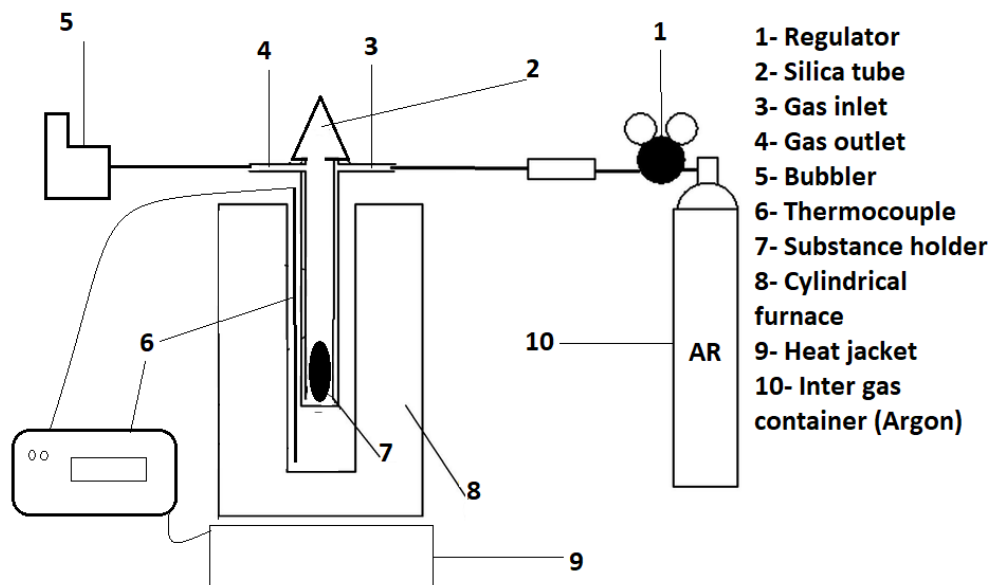


**Figure 3.15.** Diagram of  $\text{MgB}_2$  Test and Production Appliances

The silica tube was then heated to  $400\text{ }^\circ\text{C}$  within 3h and annealed for 1h. Argon gas was passed through the reaction vessel to remove oxygen and moisture and the purge was maintained until the reaction was finalized. The obtained powder was blended in a tumbler with the stoichiometric amount of Mg for the doping reaction and the mixture placed in a steel ampoule. The latter was inserted in a protective silica tube and heated in 3h to  $800\text{ }^\circ\text{C}$ , sintered for 6h and cooled down to room temperature over a period of 12h. Again argon gas was purged through the apparatus to avoid contact with air and moisture. Nitrogen as inert gas is not suitable, due to formation of BN at  $T > 500\text{ }^\circ\text{C}$ .

Same procedures were employed also for the DL-malic acid added version of  $\text{MgB}_2$ . Since both dopants are solid and can be converted to fine powders revealing only slight differences in the decomposition temperature.

The C-doped  $\text{MgB}_2$  specimens were investigated by X-ray diffraction analysis with respect to small but significant changes of their lattice constant due to carbon doping. Particularly the  $a$ -axis seemed to be very sensitive to dopants on B site, as will be explained in the next chapter.

## 4. RESULT AND DISCUSSION

In this thesis, two different precursors were used to produce carbon doped  $\text{MgB}_2$  powder: carbon based sugar and malic acid. Both substances were thermally decomposed and the grade of decomposition was analyzed by Thermogravimetric Analysis (TGA).

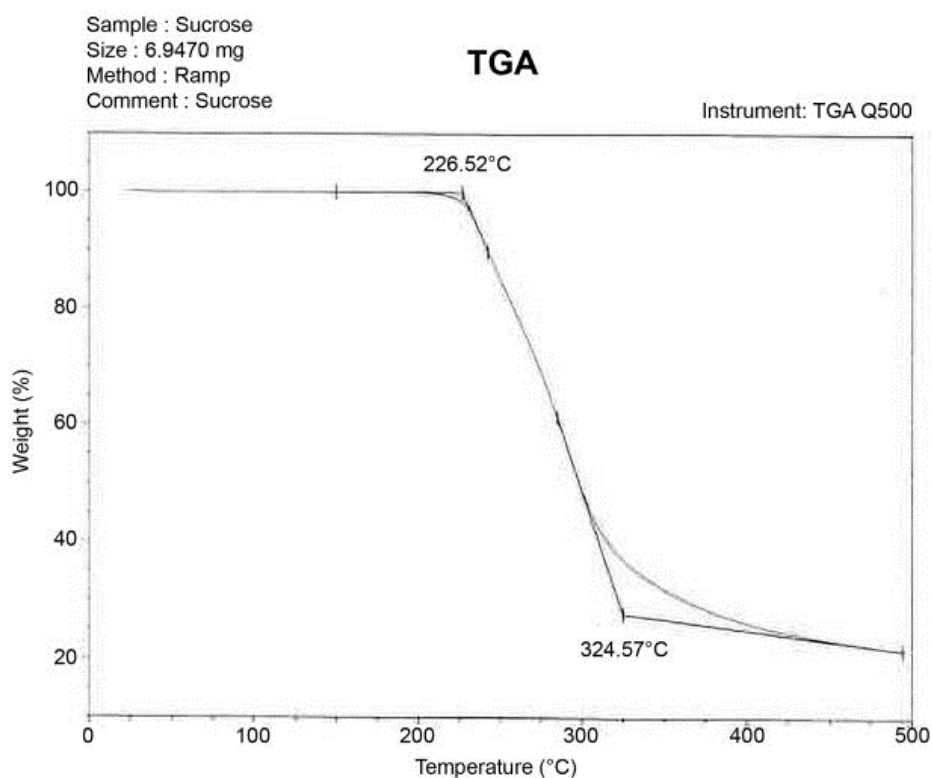


**Figure 4.16.** TGA Graph of Commercial Sugar. (“Thermal Decomposition of Sucrose in Nitrogen Atmosphere | Lamentations on Chemistry,” 2008)

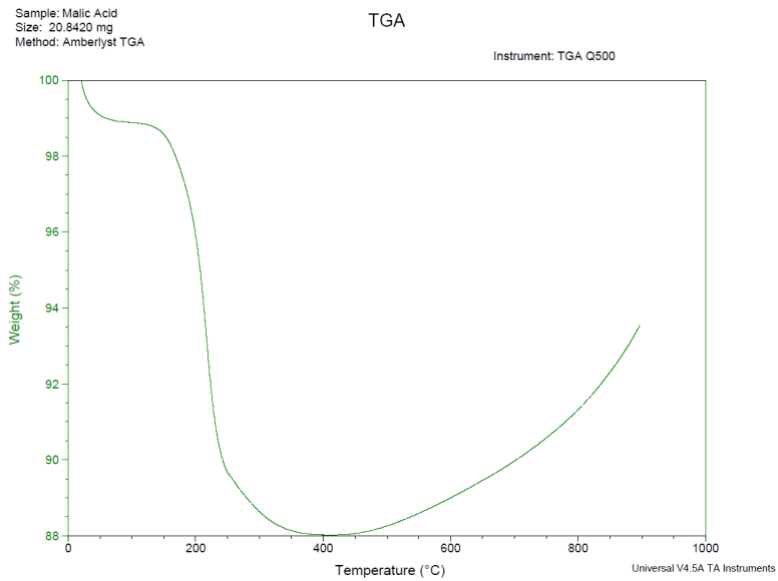


**Figure 4.17.** TGA Graph of Malic Acid

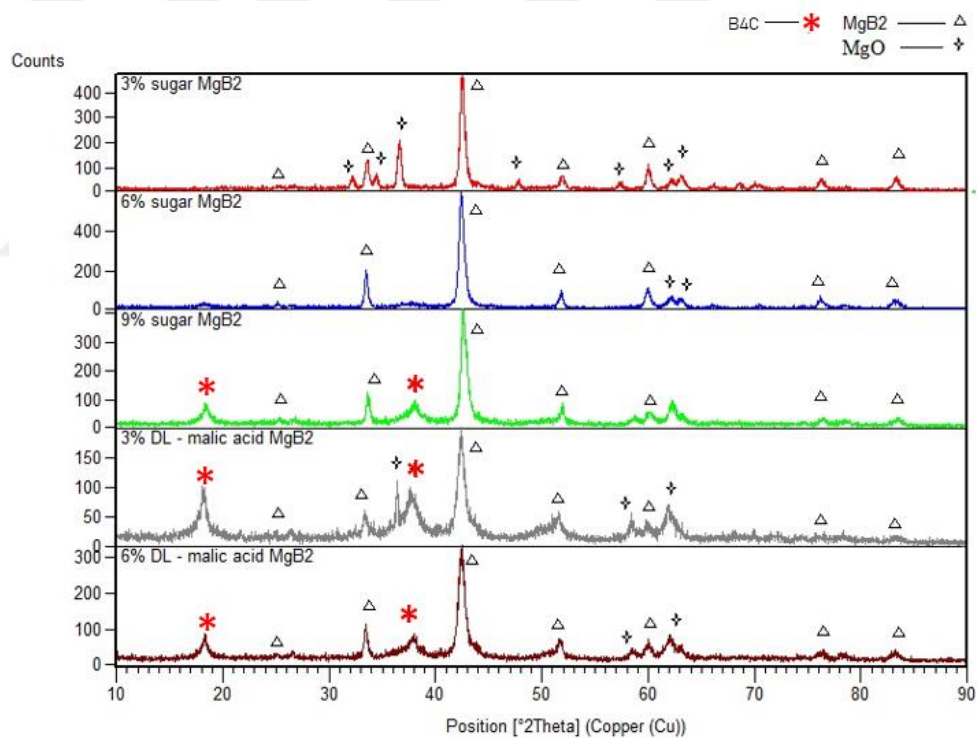


**Figure 4.18.** XRD diagrams of all C-doped MgB<sub>2</sub> powders.

It can be seen on figure 4.18 that even with argon gas there can be some oxygen impurities and also some unreacted possible B<sub>4</sub>C formations marked with red star.

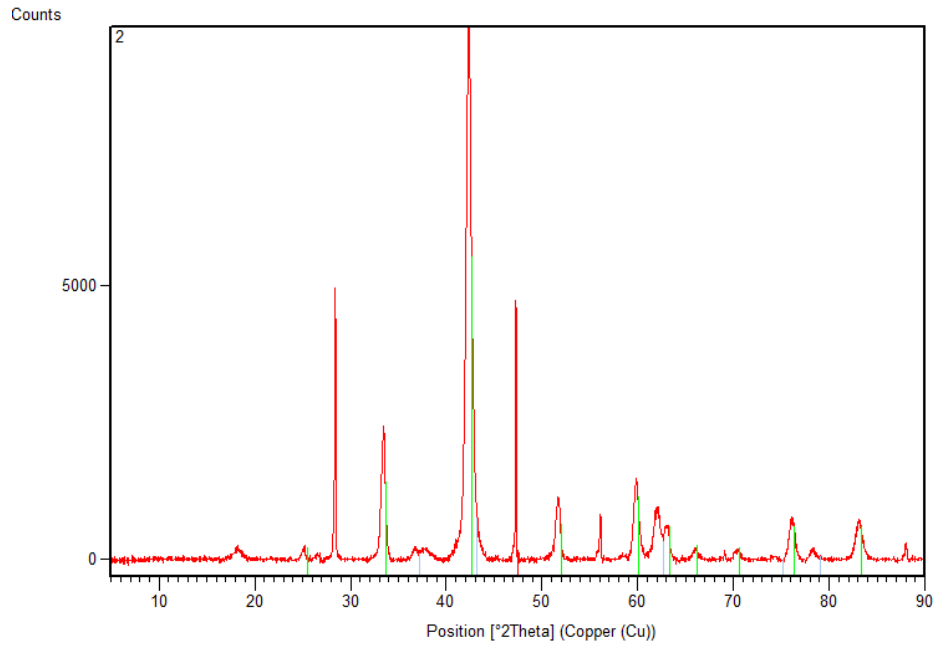


**Figure 4.19.** XRD of 6% sugar carbon doped MgB<sub>2</sub>

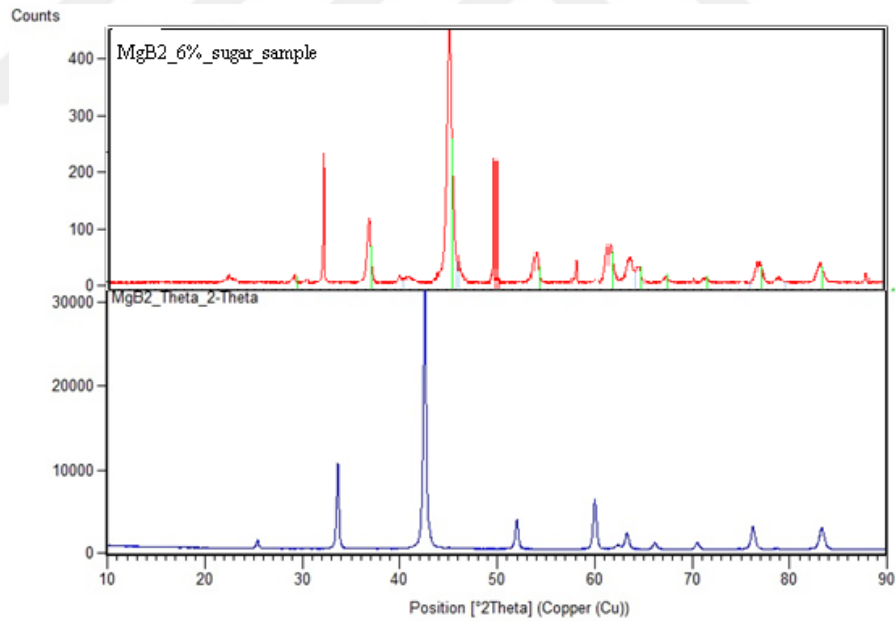


**Figure 4.20.** Comparison of the XRD patterns of MgB<sub>2</sub>

There are no obvious differences between the XRD patterns of carbon doped MgB<sub>2</sub> and its non-doped peer, slight but significant shifts in the peak positions resulting from changes in lattice parameters.

The accuracy of the peak shift can be observed on the figure 4.20. This can be relayed to the use of a standard in order to see the peak shift accurately. In our XRD measurements we used Si for a standard to separate peaks from the pure MgB<sub>2</sub>. In all our XRD measurements we used Si as a standard to locate peak shifts in this experiment.

**Table 4.7.** Carbon doping with sugar of MgB<sub>2</sub> and yield in grams.

No	Specification	Sugar %	B in gram G	Sugar in gram		Before Nominal	After Real	Yield %
				G	G			
1	1h mill – 400C°	3	0,94	0,2	1,14	1	71,15	
2	1h mill – 400C°	6	0,94	0,4	1,34	1,06	79,10	
3	1h mill – 400C°	9	0,94	0,6	1,54	1,12	72,75	

**Table 4.8.** Carbon doping with DL-Malic acid of MgB<sub>2</sub> and yield.

No	Specification	Malic acid %	B in gram G	MAcid in gram g	Before Theoretical gram	After Real gram	Yield %
2	1h mill – 400C°	6	0,94	1,36	2,3	1,06	46,09

Regarding the results of the initial decomposition given in Tab.4.3 and 4.4, the C-content of the sugar results are considerably higher than those of maleic acid. This proves that insertion of carbon into boron and MgB<sub>2</sub>, respectively, seems to be

more readily and straight forward when sugar is employed as carbon precursor. Furthermore, sugar is cheaper and more convenient.

After doping, Rietveld refinement was employed for the analysis of the changes in lattice parameters  $a$  and  $c$  which are directly related to the amount of C-doping. Prior to the refinement, the respective  $d$  and  $2\theta$  values of the *undoped*  $\text{MgB}_2$  were directly taken from the literature (Abe et al., 2009) and used. The most relevant  $d$  values are stemming from the planes (100), (101) and (002). The relationship between  $d$ -spacing and lattice constants in a hexagonal unit cell is given in (1) [38]. The  $2\theta$  values for 100 and 002 peaks are directly related to  $a$  and  $c$  axes, respectively, thus using the formula (1) next page the lattice parameter values for  $a$  and  $c$  were calculated. As mentioned above, the change of the lattice constants in the carbon doped  $\text{MgB}_2$  samples with respect to the pure magnesium diboride can easily be derived from the shift of  $2\theta$  values of the XRD diagrams of the specimen depicted in figures 6-7.

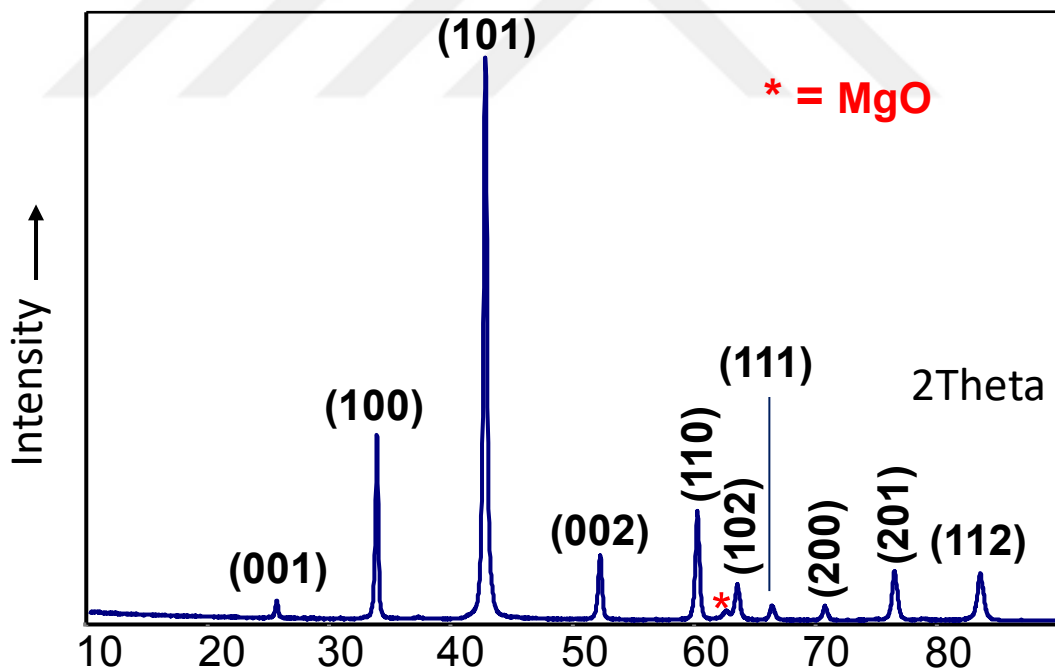


**Figure 4.21.** Miller indices for  $\text{MgB}_2$

For the lattice parameter calculations, Rigaku software was employed. Every % of carbon doping is calculated by the equation below (1).  $2\theta$  values are selected from XRD powder patterns and corresponding  $d$  values are inserted into the

equation. For  $hkl = 100$ ,  $l^2/c^2$  is equal to 0, and for  $hkl = 002$ ,  $(h^2 + hk + k^2) / a^2$  is equal to 0, enabling the calculation of  $a$  and  $c$  lattice parameters for these specific planes. For instance, 3% sugar MgB<sub>2</sub> lattice parameters are calculated as follows;

$$\frac{1}{d^2} = \frac{4}{3} \left( \frac{h^2+hk+k^2}{a^2} \right) + \frac{l^2}{c^2} \quad (1)$$

$$c = \frac{\sqrt[2]{3a^2d^2}}{\sqrt[2]{3a^2 - \sqrt[2]{4d^2}}}$$

$a = 3,091$  for  $2\theta$  42,52 degree

$d = 2,124$  for  $2\theta$  42,52 degree

Here we find  $c = 3,490$

**Table 4.9.**  $a$  and  $c$  lattice parameters of substances.

Substance	$a$	$c$	%
<b>3% sugar MgB<sub>2</sub></b>	3,091	3,490	3
<b>6% sugar MgB<sub>2</sub></b>	3,084	3,525	6
<b>9% sugar MgB<sub>2</sub></b>	3,068	3,522	9
<b>3% DL – malic acid MgB<sub>2</sub></b>	3,095	3,519	3
<b>6% DL – malic acid MgB<sub>2</sub></b>	3,088	3,520	6

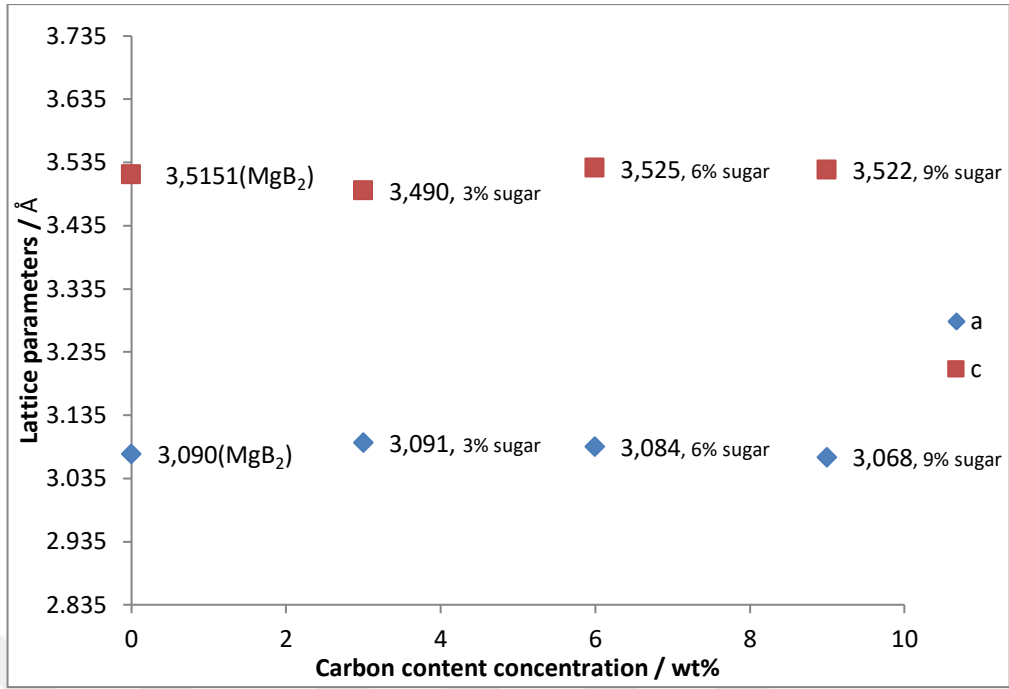


**Figure 4.22.** The lattice parameters of carbon (sugar) doping of MgB<sub>2</sub>

In figure 4.22, as the concentration increase so does the a and c parameter in the lattice accordingly due to C changing the crystal structure as it substitutes MgB<sub>2</sub>

It is a well-known phenomenon that doping MgB<sub>2</sub> with C has a drastic negative effect of its critical temperature  $T_c$  coupled with an increase of the critical current density  $J_c$  on higher fields (Mickelson, Cumings, Han, & Zettl, 2002). Furthermore, it has also been reported that MgB<sub>2</sub> superconducting temperature decreases with applied pressure; i.e.  $T_c$  decreases along with the reduction of the lattice constants (Buzea & Yamashita, 2001). In the figure 4.20 we see the comparison of the XRD patterns of the undoped MgB<sub>2</sub> vs sugar and doped ones with a C content of 3%-, 6%- and 9%-wt. Despite small errors, it can be clearly seen that for both dopants the c axis remains almost invariant. In contrast to the marginal shift of a axis of only 0.002 Å (3.090 Å -3.088 Å) in the malic acid case, the difference for sugar-doped samples is markedly: 0.026Å (3.090 Å -3.064 Å).



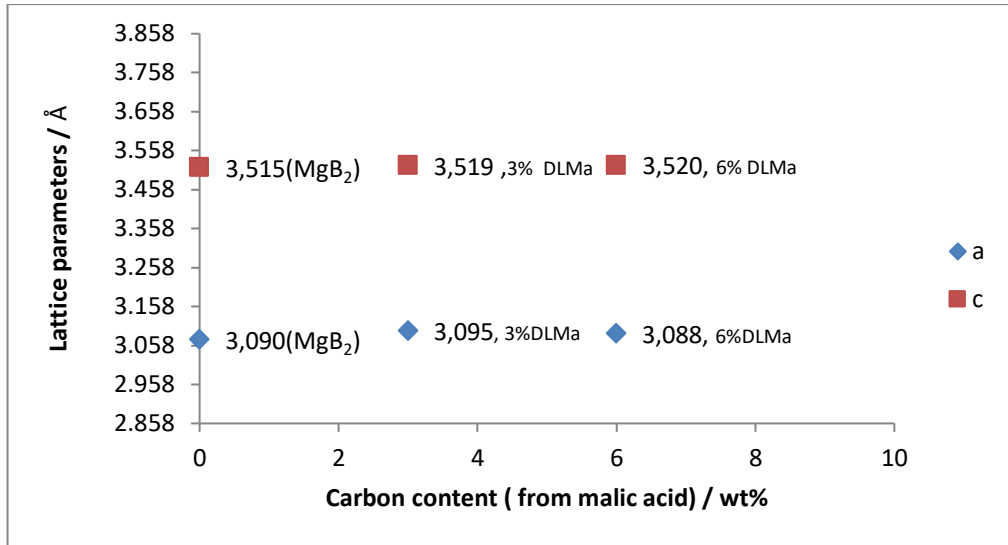


**Figure 4.23.** The malic acid assisted version of the C doping method

Above shown the yield in terms of %wt carbon inside the final product as much as sugar does, still have at least 65% of its carbon content transferred to final product in MgB<sub>2</sub>.

During the C doping into MgB<sub>2</sub>, the carbon atoms can migrate into the boron sites or into interstitial positions within boron rings and grain boundaries. It is reported that the very small changes observed for the *c* axis in doped samples are related to C substitution into the holes of the 6-membered boron rings. Therefore, we can assume that the real C doping into B sites and the nominal C concentration, which is the theoretical amount of added C, and the terms nominal and real are used in the literature to separate them. Various methods are reported to calculate the real C concentration *x* (Batani et al., 2015).

$$x = 7,5 \left( \Delta \left( \frac{c}{a} \right) \right)$$

Hereby  $\Delta (c/a)$  is the difference between the *c/a* ratio of C-doped samples and the *c/a* ratio of undoped sample,  $\Delta_{(c-a)}$  corresponds to:

$$\Delta_{(c-a)} = \left( \frac{c}{a} \right)_{undoped} - \left( \frac{c}{a} \right)_{doped}$$

Using the experimental data for *a* and *c* for pure and 6% sugar doped MgB<sub>2</sub>, one obtains for undoped sample:

$$\Delta_{(c-a)} = \frac{3,515}{3,090} - \frac{3,525}{3,084} = 0,002$$

$$x = 7,5 * 0,002 = 0,015$$

From this result, we can see that the “real” and “nominal” concentrations are  $1,5 \cdot 10^{-2}$  and  $6 \cdot 10^{-2}$ , respectively, meaning that ca. 25% of the theoretically measured carbon is inserted into the  $\text{MgB}_2$  lattice. Using the above equation, one obtains for the 6% malic acid doped sample  $x = 0.008$ . The latter finding confirms that in this case the real carbon concentration in the  $\text{MgB}_2$  specimen is ca. 12%, approximately half of the amount calculated for the sugar based one. The significant differences in the carbon contents between the malic acid and sugar based C-doping experiments are very likely due to the homogeneity of the overall process. There are no other effects since all doping reactions were performed under the same temperature and pressure conditions and no other element was used. Thus the slight but significant changes in lattice parameters can be explained by different homogeneity and small experimental errors. As summary, can say that substitution of carbon into  $\text{MgB}_2$  would decrease the lattice parameter  $a$  while the  $c$  parameter practically doesn't alter so that overall one observes an increase of the  $c/a$  ratio the lattice constants which is proportional to the amount of carbon inserted into the  $\text{MgB}_2$  lattice.

## 5. CONCLUSION AND RECOMMENDATIONS

In the present study, five samples of carbon doped MgB<sub>2</sub> compounds are synthesized three of them with sugar and two with DL-Malic acid by means of cylindrical furnace and conventional methods. Also, it is seen that sugar starter shows greater yields than the DL-Malic acid on decomposition. All samples are characterized via BRUKER XRD machine. Additionally, how much of the carbon is reacted with the MgB<sub>2</sub> is checked and excess formation of MgO and B<sub>4</sub>C products reported which also can conclude less than inserted amount is obtained.

From figure 4.16 we can see the amount of C produced when 6.9470mg sucrose is being burnt. Remaining carbon content after its initial decomposition is the carbon substance that we acquire from burning our sugar or malic acid in the furnace at 400 °C. Unfortunately, there are no easy methods doing these aside from putting carbon containing contents one by one into the furnace then taking them out and mixing with B and Mg then to put back once again to synthesize MgB<sub>2</sub>. This method is fast yet even with an inert gas in presence; Oxygen always reacts with the sample contents.

Table 4.7 and 4.8 clearly shows that carbon doped MgB<sub>2</sub> whose starting material is sugar has a lot better reaction in terms of yield. Although both carbon containing substances fairly easy to obtain and handle, sugar is dominating with a little margin which can be explained as having a better decomposition and reaction ratio with given Mg and B in furnace at 800 °C. Table 4.9 shows the lattice parameters of a C doped MgB<sub>2</sub>. Figure 4.22 and Figure 4.23 shows the differences between doped and non-doped version of lattice parameters and the shift when C inserted in MgB<sub>2</sub>. This shift can be explained by changes in a and c lattice parameters due to change in crystal structure when C fills the Boron vacancies.

To sum up, we have tested the best way to dope MgB<sub>2</sub> with carbon to get highest yield and easiest method in terms of industrial production in between malic acid and sugar. Crystal structure and lattice parameter a and c it is found that sugar is a better candidate for its reaction % and its yield overall.

## 6. REFERENCES

- Abe, H., Miyazoe, A., Kurashima, K., Nakajima, K., Aoyagi, T., Nishida, K., ... Wada, H. (2009). "Highly crystalline superconducting MgB<sub>2</sub> nanowires formed by electrodeposition." *Advanced Materials*, (June 2009), 1–16.
- T. Arai, (2015) "Agglomeration of Powder" - an overview | ScienceDirect Topics. <https://www.sciencedirect.com/topics/materials-science/agglomeration-of-powder> 2 May 2019
- Alecu, G., Stancu, N., Zamfir, S., & Cosac, A. (2007). "Superconducting properties of MgB<sub>2</sub> materials." 9(4), 1187–1189.
- Bateni, A., Erdem, E., Repp, S., Acar, S., Kokal, I., Häbler, W., ... Somer, M. (2015). "Electron paramagnetic resonance and Raman spectroscopy studies on carbon-doped MgB<sub>2</sub> superconductor nanomaterials." *Journal of Applied Physics*, 117(15).
- Buzea, C., & Yamashita, T. (2001). "Review of superconducting properties of." 1–35.
- Cooley, L. D., Ghosh, A. K., & Scanlan, R. M. (2005). "Costs of high-field superconducting strands for particle accelerator magnets." *Superconductor Science and Technology*, 18(4).
- Giunchi, G., Ripamonti, G., Raineri, S., Botta, D., Gerbaldo, R., & Quarantiello, R. (2004). "Grain size effects on the superconducting properties of high density bulk MgB<sub>2</sub>." *Superconductor Science and Technology*, 17(9), S583–S588.
- Guan, M., Wang, X., & Zhou, Y. (2015). "Effects of cold-treatment and strain-rate on mechanical properties of NbTi/Cu superconducting composite wires." *SpringerPlus*, 4(1), 1–7.
- L. David Roper, (2016) "Helium Depletion" <http://www.roperld.com/Science/minerals/Helium.htm> 2 May 2019
- Adam Augustyn, (2019) "High-Tc superconductor" <https://www.britannica.com/science/high-Tc-superconductor> 24 July 2019
- High, N., & Field, M. (2001). "Superconductivity at 49 K in copper doping magnesium diboride." *Nature*, 410(March), 1–3.
- Kim, J. H., Zhou, S., Hossain, M. S. A., Pan, A. V, & Dou, S. X. (2006). "Strong enhancement of critical current density in MgB<sub>2</sub> superconductor using carbohydrate doping." *Applied Physics Letters*, 89, 142505.

- Klug, H. ., & Alexander, L. E. (1974). "X-ray Diffraction Procedures for Polycrystalline and Amorphous Materials." Wiley, 366.
- Kornbluth, P. (2019). "Helium Shortage 3.0": (February 2018), 2018–2020.
- Kovalenko, A. N. (2017). "High-temperature superconductivity: From macro- to nanoscale structures." *Nanosystems: Physics, Chemistry, Mathematics*, 7(6), 941–970.
- Larbalestier, D. C. (1980). "Nb-Ti Alloy Superconductors—Present Status and Potential for Improvement." In *Advances in Cryogenic Engineering Materials* (pp. 10–36).
- Larminie, J., & Dicks, A. (2003). "Fuel cell systems explained." In *Fuel*.
- Li, W., & Dou, S. (2010). "Superconducting Properties of Carbonaceous Chemical Doped MgB<sub>2</sub>." (August 2015).
- Loh, Z. H., Samanta, A. K., & Sia Heng, P. W. (2014). "Overview of milling techniques for improving the solubility of poorly water-soluble drugs." *Asian Journal of Pharmaceutical Sciences*, 10(4), 255–274.
- Mickelson, W., Cumings, J., Han, W. Q., & Zettl, A. (2002). "Effects of carbon doping on superconductivity in magnesium diboride." 65, 2–4.
- Müller, C. B., & Saur, E. J. (1964). "Influence of pressure on the superconductivity of some high-field superconductors." *Reviews of Modern Physics*, 36(1), 103–105.
- Nishijima, G., Watanabe, K., Murase, S., Katagiri, K., & Iwaki, G. (2005). "Superconducting properties and thermal stability of high-strength Nb 3Sn wire with ta-reinforced filaments." *IEEE Transactions on Applied Superconductivity*, 15(2 PART III), 3442–3445.
- Sawada, M., Shimoyama, J., Takagi, N., Motoki, T., Kodama, M., & Tanaka, H. (2018). "A new carbon source MgB<sub>2</sub>C<sub>2</sub> for the synthesis of carbon-doped MgB<sub>2</sub> materials." *Solid State Communications*.
- Silva-Guillén, J. A., Noat, Y., Cren, T., Sacks, W., Canadell, E., & Ordejón, P. (2015). "Tunneling and electronic structure of the two-gap superconductor MgB<sub>2</sub>." *Physical Review B - Condensed Matter and Materials Physics*, 92(6), 1–7.
- The Advantages and Disadvantages of Liquid Hydrogen 2018 - "Liquid Hydrogen vs. Fossil Fuels."  
<https://www.sites.google.com/site/liquidhydrogenvsfossilfuels/the-advantages-and-disadvantages-of-liquid-hydrogen> 4 May 2019

- The thermal conductivity of gases "Electronics Cooling." (1998)  
<https://www.electronics-cooling.com/1998/09/the-thermal-conductivity-of-gases/> 12 May 2019
- Thermal Decomposition of Sucrose in Nitrogen Atmosphere (2008) | "Lamentations on Chemistry." <https://gaussling.wordpress.com/2008/10/04/thermal-decomposition-of-sucrose/> 2 May 2019
- Tolga, A., & Ibrahim, U. (2016). "The Effect of Fe Diffusion on Some Physical and Superconducting Properties of MgB<sub>2</sub>." *Journal of Superconductivity and Novel Magnetism*.
- Troyanov, S. I., Boltalina, O. V., Kouvytchko, I. V., Troshin, P. A., Kemnitz, E., Hitchcock, P. B., & Taylor, R. (2002). "Molecular and crystal structure of the adducts of C<sub>60</sub>F<sub>18</sub> with aromatic hydrocarbons." *Fullerenes Nanotubes and Carbon Nanostructures*, 10(3), 243–259.
- Vajpayee, A., Kishan, H., Narlikar, A. V, Road, K., Bhalla, G. L., Delhi, N., & Wang, X. L. (2007). "HIGH FIELD PERFORMANCE OF NANO-DIAMOND DOPED MgB<sub>2</sub>." 1–12.
- Xu, X., Kim, J. H., Yeoh, W. K., Zhang, Y., & Dou, S. X. (2006). "Improved J<sub>c</sub> of MgB<sub>2</sub> superconductor by ball milling using different media." *Superconductor Science and Technology*, 19(11).
- Yao, W., Bascuñán, J., Kim, W.-S., Hahn, S., Lee, H., & Iwasa, Y. (2008). "A Solid Nitrogen Cooled MgB<sub>2</sub> Coil for MRI Applications." *IEEE Transactions on Applied Superconductivity : A Publication of the IEEE Superconductivity Committee*, 18(2), 912–915.
- Zhou, S., Pan, A. V., Wexler, D., & Dou, S. X. (2007). "Sugar coating of boron powder for efficient carbon doping of MgB<sub>2</sub> with enhanced current-carrying performance." *Advanced Materials*, 19(10), 1373–1376.



# **APPENDICES**

## 7. APPENDICES

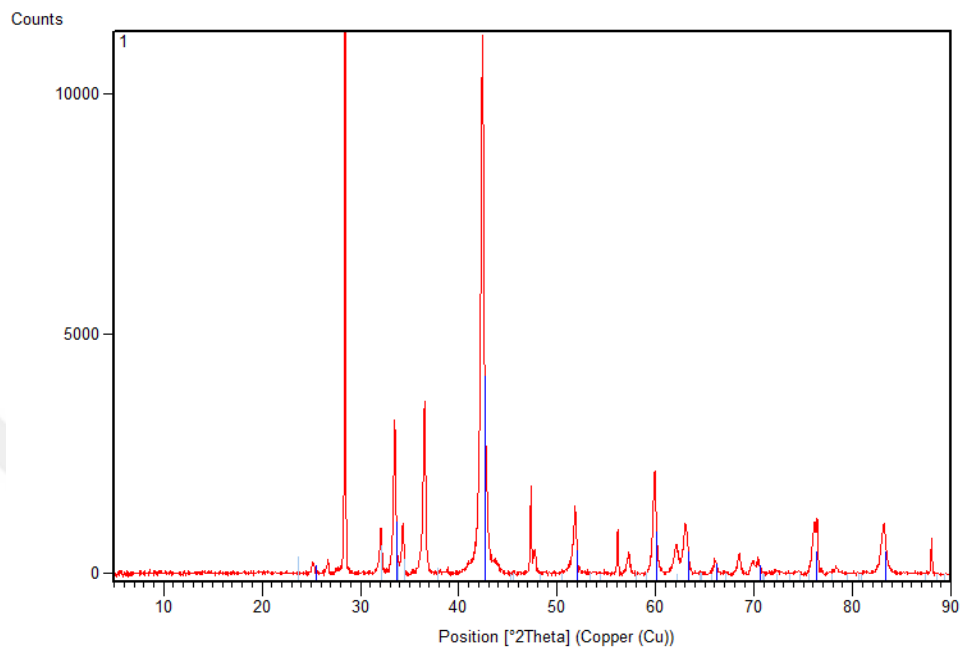


**Figure 7.24.** XRD of sample no:1 3% carbon doped (Sugar) MgB<sub>2</sub>

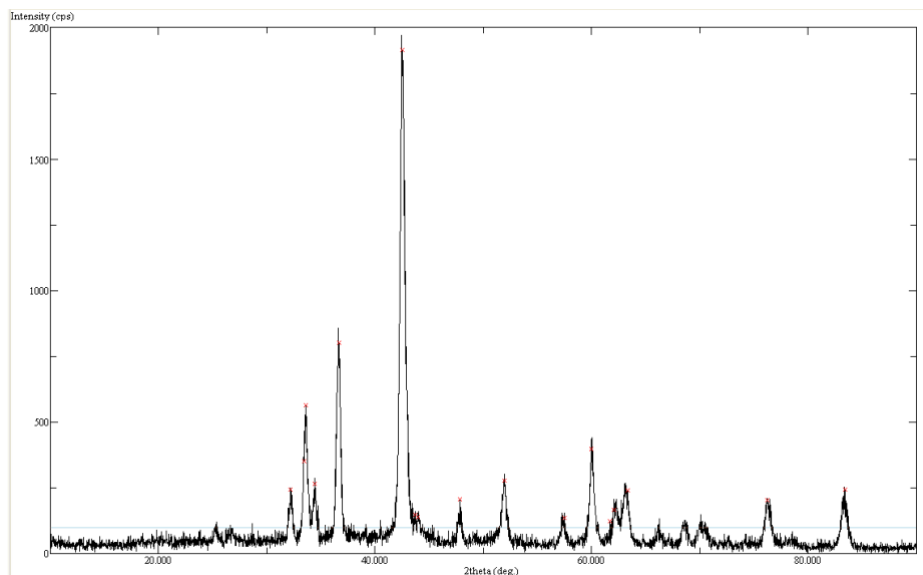


**Figure 7.25.** Rietveld analysis of 3% carbon (Sugar) doped MgB<sub>2</sub>



**Table 7.10.** Rietveld analysis of 3% carbon doped (Sugar) MgB<sub>2</sub>

Sample-1-3%	2theta	d-value
1	32.200	2,777
2	33.500	2,677
3	33.640	2,661
4	34.480	2,599
5	36.680	2,448
6	42.520	2,124
7	43.720	2,068
8	44.000	2,056
9	47.860	1,899
10	51.960	1,758
11	57.520	1,600
12	60.020	1,540
13	61.700	1,502
14	62.080	1,493
15	63.340	1,467
16	76.260	1,247
17	83.420	1,157

**Table 7.11.** Lattice parameters calculated from (Klug & Alexander, 1974)

a	c	%carbon
3,091	3,490	3

**Table 7.12.** Result from LECO Carbon analyzer 3% carbon doped (Sugar)

Bileşen (Component)	Birim (Unit)	Spektler (Specs)	Sonuçlar (Results)
C	%		2,71

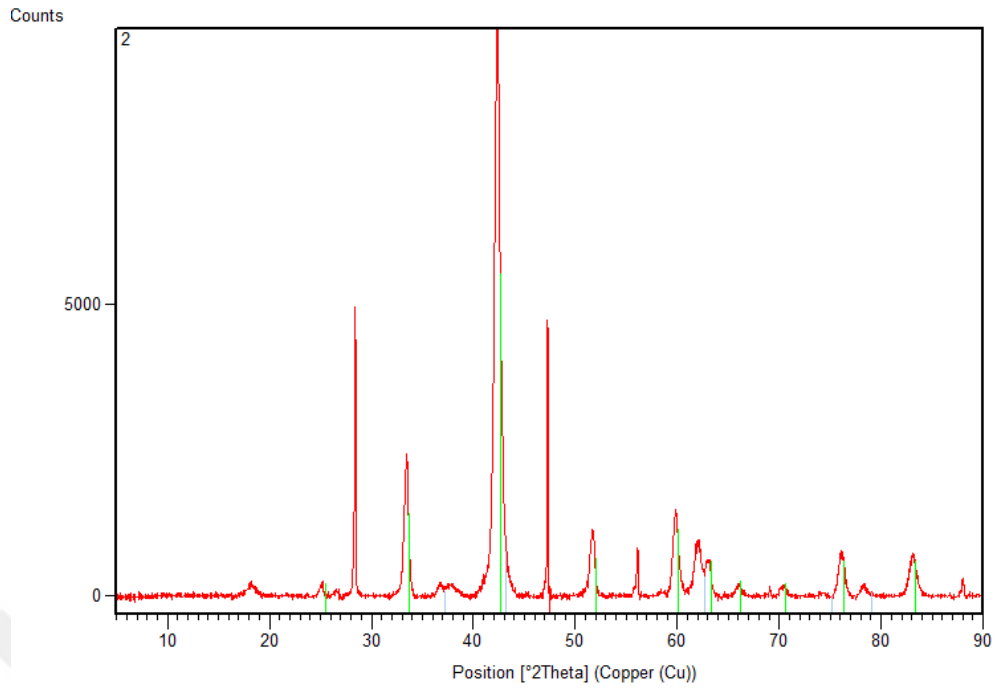


**Figure 7.26.** XRD of sample no: 2, 6% carbon doped (Sugar) MgB<sub>2</sub> sample.

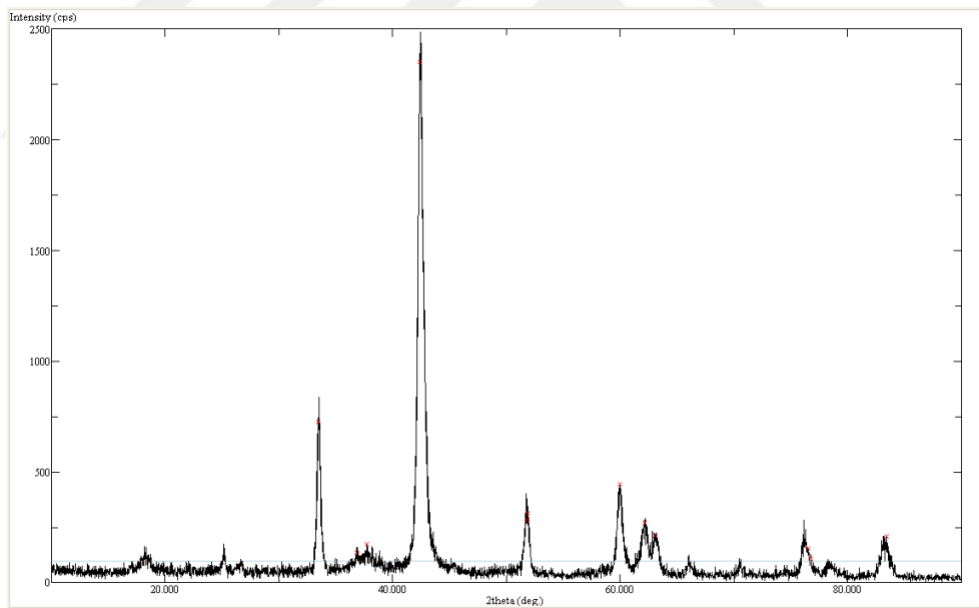


**Figure 7.27.** Rietveld analysis of 6% carbon doped (Sugar) MgB<sub>2</sub> sample.

**Table 7.13.** Rietveld analysis of 6% carbon doped (Sugar) MgB<sub>2</sub>.

<b>Sample-2-6%</b>	<b>2theta</b>	<b>d-value</b>
<b>1</b>	<b>33.520</b>	2,671
<b>2</b>	36.860	2,436
<b>3</b>	37.720	2,382
<b>4</b>	<b>42.420</b>	2,129
<b>5</b>	51.800	1,763
<b>6</b>	<b>51.900</b>	1,760
<b>7</b>	59.980	1,541
<b>8</b>	62.160	1,492
<b>9</b>	63.040	1,473
<b>10</b>	76.580	1,243
<b>11</b>	76.780	1,240
<b>12</b>	83.480	1,157

**Table 7.14.** Lattice parameters calculated from (Klug & Alexander, 1974)

<b>a</b>	<b>c</b>	<b>%carbon</b>
<b>3,084</b>	<b>3,525</b>	<b>6</b>

**Table 7.15.** Result from LECO Carbon analyzer 6% carbon doped (Sugar)

<b>Bileşen (Component)</b>	<b>Birim (Unit)</b>	<b>Spektler (Specs)</b>	<b>Sonuçlar (Results)</b>
C	%		4,50

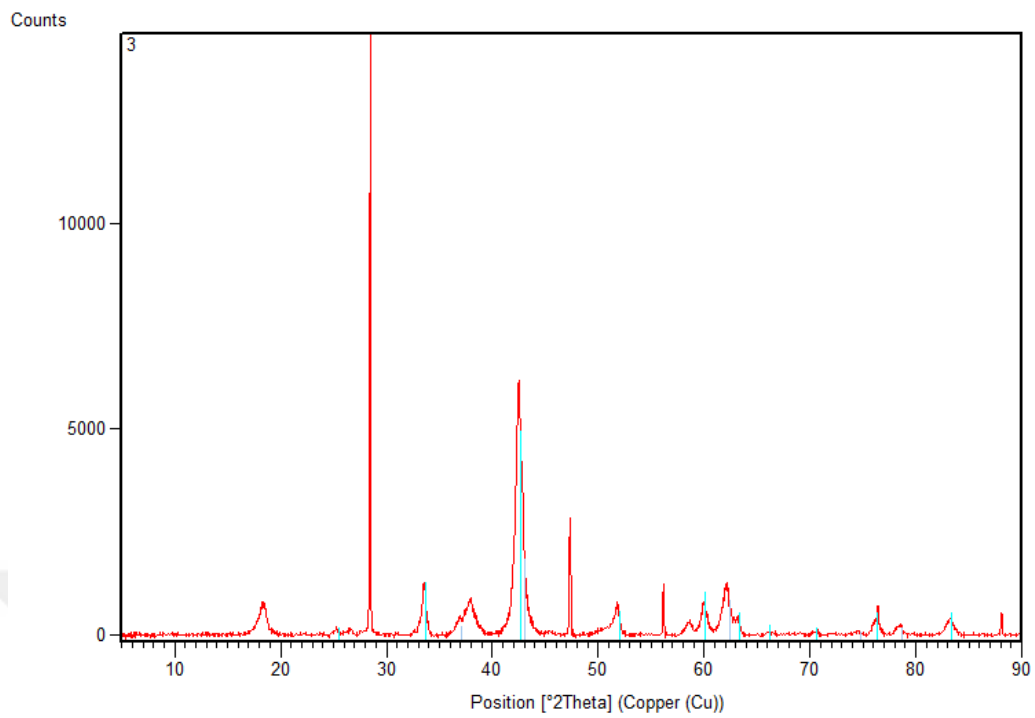


**Figure 7.28.** XRD of sample no: 3, 9% carbon doped MgB<sub>2</sub> (Sugar) sample.

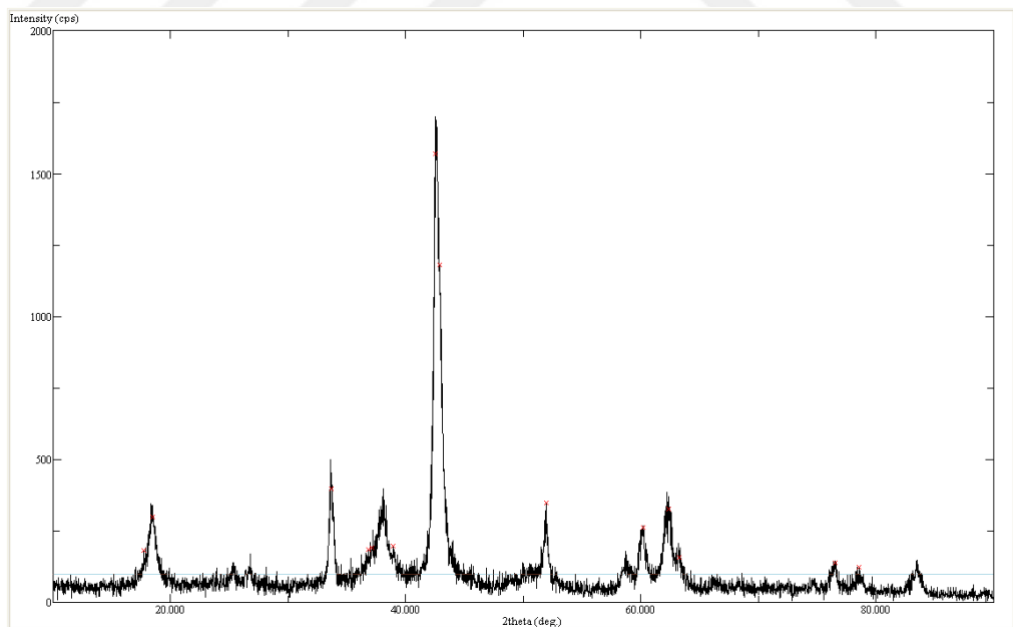


**Figure 7.29.** Rietveld analysis of 9% carbon doped (Sugar) MgB<sub>2</sub>

**Table 7.16.** Rietveld analysis of 9% carbon doped (Sugar) MgB<sub>2</sub>

Sample-3-9%	2theta	d-value
1	17.780	4,984
2	18.840	4,797
3	33.700	2,657
4	36.840	2,537
5	37.180	2,416
6	38.960	2,309
7	42.580	2,121
8	42.920	2,105
9	52.000	1,757
10	60.220	1,535
11	62.400	1,486
12	63.260	1,468
13	76.540	1,243
14	78.540	1,216

**Table 7.17.** Lattice parameters calculated from (Klug & Alexander, 1974)

a	c	%carbon
3,068	3,522	9

**Table 7.18.** Result from LECO Carbon analyzer 9% carbon doped (Sugar)

Bileşen (Component)	Birim (Unit)	Spektler (Specs)	Sonuçlar (Results)
C	%		5,43

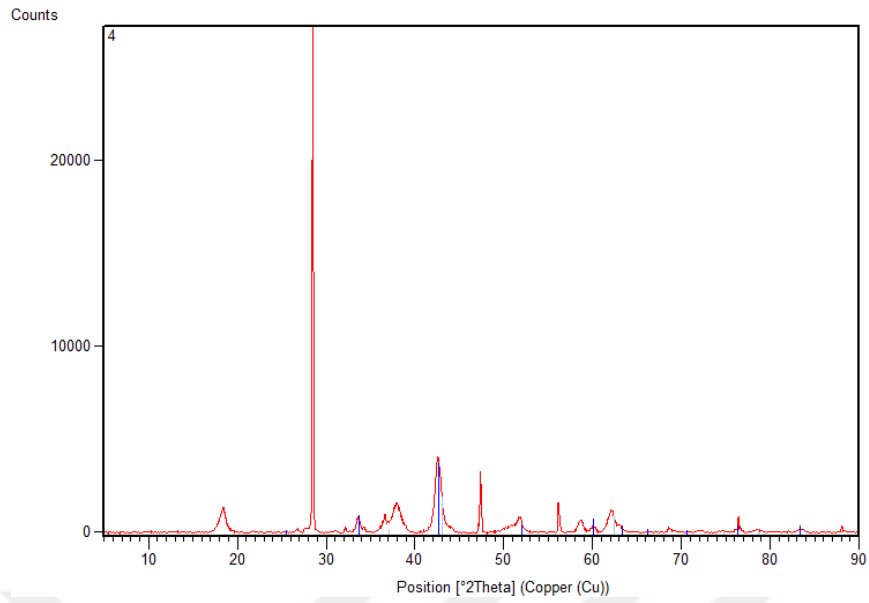


**Figure 7.30.** XRD of sample no: 4, 3% carbon doped with malic acid

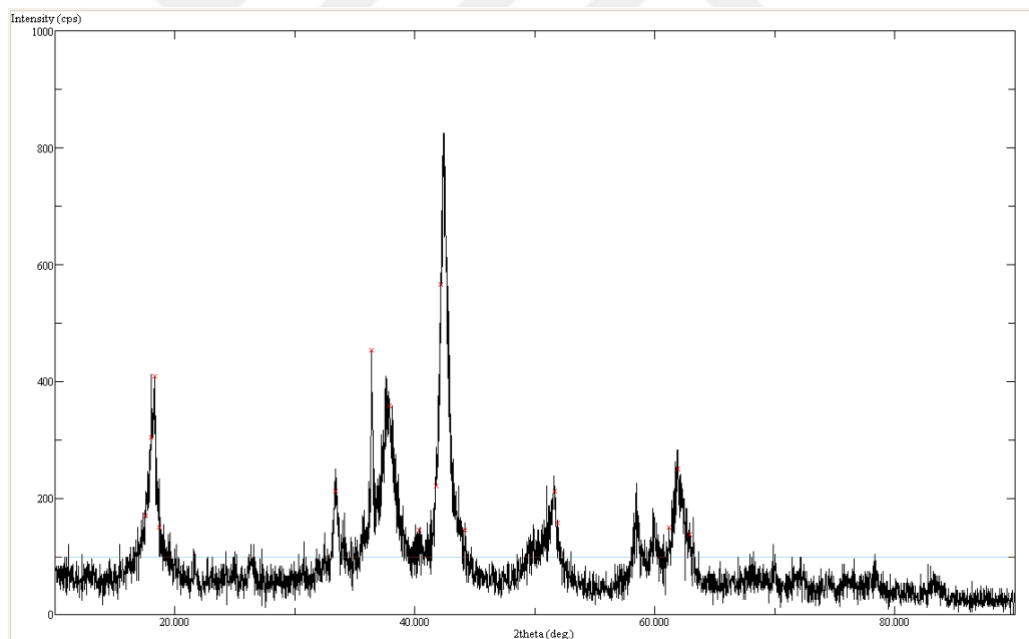


**Figure 7.31.** Rietveld analysis of 3% carbon doped (Malic Acid) MgB<sub>2</sub>

**Table 7.19.** Rietveld analysis of 3% carbon doped MgB<sub>2</sub> (Malic Acid)

Sample-4- 3%MA	2theta	d-value
1	17.620	5,029
2	18.080	4,902
3	18.300	4,833
4	18.700	4,741
5	33.400	2,680
6	36.420	2,464
7	37.940	2,369
8	40.400	2,230
9	41.800	2,159
10	42.200	2,139
11	44.200	2,047
12	51.660	1,767
13	51.920	1,759
14	61.220	1,512
15	61.920	1,497
16	62.920	1,475

**Table 7.20.** Lattice parameters calculated from (Klug & Alexander, 1974)

a	c	%carbon
3,095	3,519	3

**Table 7.21.** Result from Carbon analyzer 3% carbon doped Malic Acid

Bileşen (Component)	Birim (Unit)	Spektler (Specs)	Sonuçlar (Results)
C	%		2,29

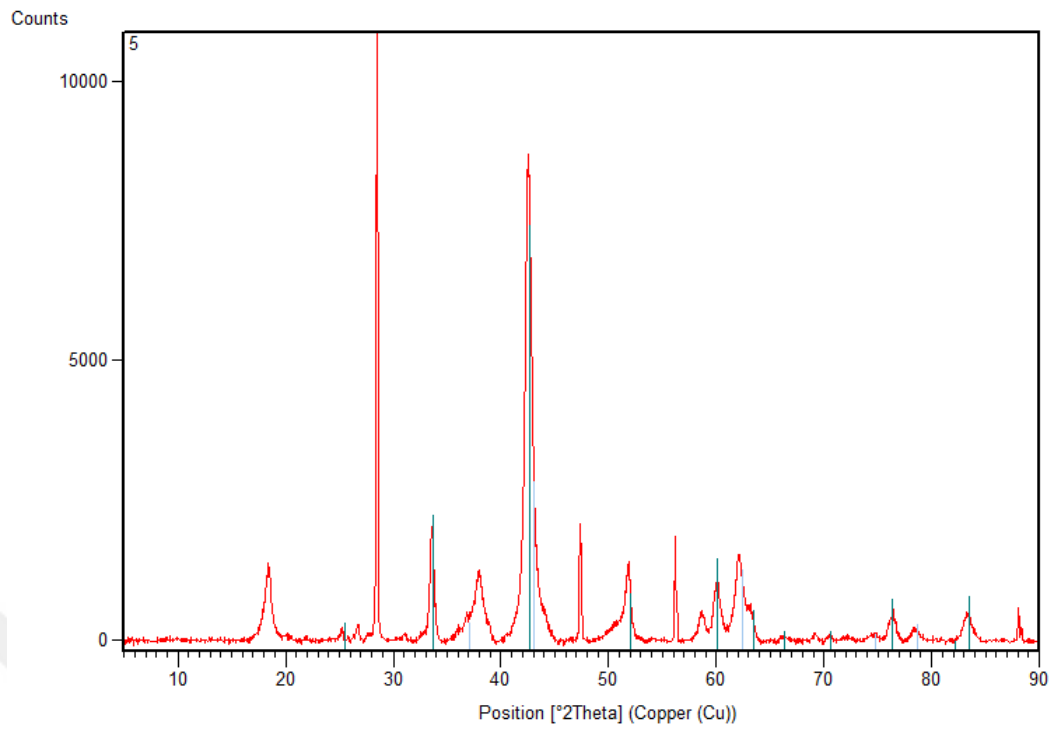


**Figure 7.32.** 6% carbon doped with malic acid addition MgB<sub>2</sub> sample

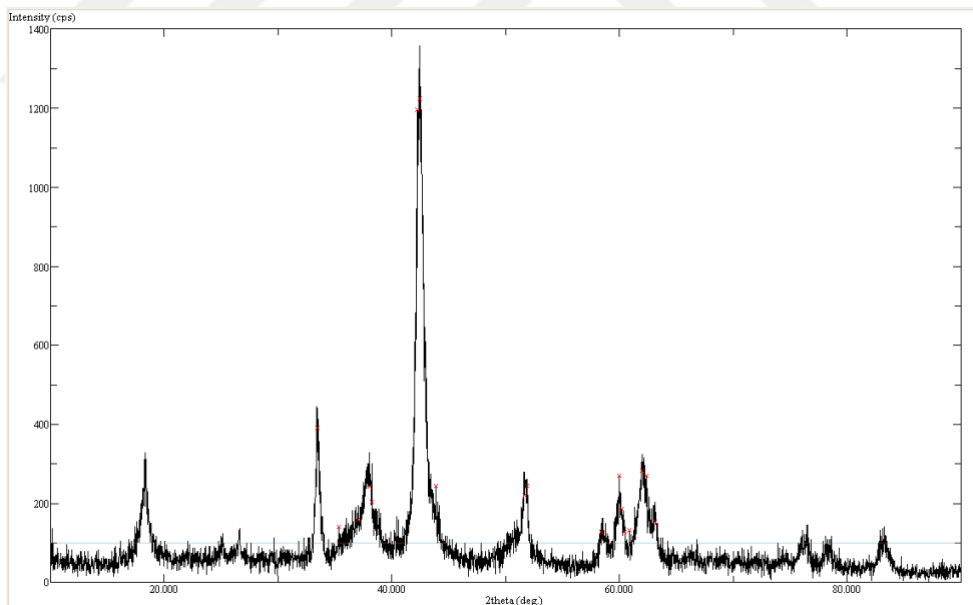


**Figure 7.33.** Rietveld analysis of 6% carbon doped (Malic Acid) MgB<sub>2</sub>



**Table 7.22.** Rietveld analysis of 6% carbon doped MgB<sub>2</sub> (Malic Acid)

Sample-5- 6%MA	2theta	d-value
<b>1</b>	<b>33.480</b>	2,674
<b>2</b>	35.340	2,537
<b>3</b>	37.040	2,425
<b>4</b>	38.060	2,362
<b>5</b>	38.300	2,348
<b>6</b>	42.280	2,135
<b>7</b>	<b>42.440</b>	2,128
<b>8</b>	43.880	2,061
<b>9</b>	51.720	1,766
<b>10</b>	<b>51.900</b>	1,760
<b>11</b>	58.440	1,577
<b>12</b>	60.020	1,540
<b>13</b>	60.200	1,535
<b>14</b>	60.440	1,530
<b>15</b>	60.900	1,519
<b>16</b>	62.000	1,495
<b>17</b>	62.360	1,487
<b>18</b>	63.160	1,470

**Table 7.23.** Lattice parameters calculated from (Klug & Alexander, 1974)

<b>a</b>	<b>c</b>	<b>%carbon</b>
<b>3,088</b>	<b>3,520</b>	<b>6</b>

**Table 7.24.** Result from Carbon analyzer 6% carbon doped Malic Acid

<b>Bileşen</b> (Component)	<b>Birim</b> (Unit)	<b>Spektler</b> (Specs)	<b>Sonuçlar</b> (Results)
C	%		2,10

## 8. CURRICULUM VITAE

**Name SURNAME** : Emir PİLTEN

**Place and Date of Birth** : Şişli / 13.08.1991

**Bachelor's Degree** : Abant İzzet Baysal University 2014

**e-mail** : emirpilten@gmail.com

**Address** : Merdivenköy/ Paksa metroport sitesi/ yekta  
sokak/no:1 A blok daire 3 Kadıköy/İstanbul